

ATMOS Version 3 water vapor measurements: Comparisons with observations from two ER-2 Lyman- α hygrometers, MkIV, HALOE, SAGE II, MAS, and MLS

H. A. Michelsen,¹ G. L. Manney,^{2,3} F. W. Irion,² G. C. Toon,² M. R. Gunson,² C. P. Rinsland,⁴ R. Zander,⁵ E. Mahieu,⁵ M. J. Newchurch,⁶ P. N. Purcell,⁷ E. E. Remsberg,⁴ J. M. Russell III,⁸ H. C. Pumphrey,⁹ J. W. Waters,² R. M. Bevilacqua,¹⁰ K. K. Kelly,¹¹ E. J. Hints,¹² E. M. Weinstock,¹³ E.-W. Chiou,⁴ W. P. Chu,⁴ M. P. McCormick,⁸ and C. R. Webster²

Abstract. We have compared a new version of ATMOS retrievals (Version 3) of stratospheric and mesospheric water vapor with observations from shuttle-, satellite-, balloon-, and aircraft-borne instruments. These retrievals demonstrate agreement to within 5% MkIV observations in the middle and lower stratosphere. ATMOS agrees with the NOAA Lyman- α hygrometer to within 5%, except for features with spatial scales less than the vertical resolution of ATMOS (such as the lower stratospheric seasonal cycle). ATMOS observations are 10-16% lower than measurements from the Harvard Lyman- α hygrometer in the lower stratosphere and 7-14% higher than those from MLS (prototype Version 0104) throughout most of the stratosphere. Agreement is within 7% with MAS (Version 20) in the middle and upper stratosphere, but differences are closer to 13% in the lower stratosphere. Throughout the stratosphere, agreement is within 8% with HALOE (Version 19). ATMOS data from 1994 show agreement with SAGE II (Version 6) values to within 8% in the middle stratosphere, but ATMOS observations are systematically higher than those from SAGE II by as much as 41% in the lower stratosphere. In contrast, ATMOS 1985 values are systematically lower than SAGE II values from sunset occultations in the lower stratosphere near 70 hPa but are in better agreement with sunrise occultations. Version 3 retrievals in the upper stratosphere and lower mesosphere are typically 5-10% lower than Version 2 values between 1 and 0.05 hPa. This reduction improves agreement with HALOE, MAS, and MLS upper atmospheric observations, but ATMOS values still tend to be higher than values from these instruments in the middle mesosphere. Agreement among the instruments compared here (except for SAGE II) is generally within 15% in the middle to lower stratosphere and

mesosphere and within 10% in the middle to upper stratosphere. At altitudes near 30 km, all instruments (including SAGE II) agree to within 10%.

1. Introduction

Recent work has suggested that stratospheric water vapor plays a role in the energy balance of the atmosphere. Increases in stratospheric humidity may enhance tropospheric warming and stratospheric cooling [Rind and Lonergan, 1995; Rind, 1995; Forster and Shine, 1999; Dvortsov and Solomon, 2001; Oinas *et al.*, 2001; Shindell, 2001; Smith *et al.*, 2001] and accelerate rates of heterogeneous reactions that initiate catalytic loss of lower stratospheric ozone [Hofmann and Oltmans, 1992; Michelsen *et al.*, 1999a]. Accurate and long term measurements of water vapor in the atmosphere are required to confirm the projected effects of changes in water vapor on climate and chemistry and to improve and validate climate models [Rind, 1995]. Satellite observations from solar occultation or limb-emission instruments are critical for mapping the distribution of water in the stratosphere, but such retrievals are difficult near and below the tropopause, where the vertical gradient in water is steep. The Atmospheric Trace Molecule Spectroscopy (ATMOS) instrument is a solar occultation space-shuttle-borne Fourier transform infrared spectrometer, which simultaneously measures vertical profiles of a variety of atmospheric species from the upper troposphere to well above the stratosphere [Farmer *et al.*, 1987; Gunson *et al.*, 1990, 1996]. This paper describes and validates a new retrieval (Version 3) of ATMOS stratospheric and mesospheric water vapor measurements. Although this new version was designed for better accuracy near and below the tropopause, improvements in H₂O retrievals are also apparent in the stratosphere and mesosphere. We compare the Version 3 stratospheric and mesospheric profiles with measurements from the National Oceanic and Atmospheric Administration (NOAA) and Harvard ER-2 Lyman- α hygrometers, the MkIV balloon instrument, the Millimeter-wave Atmospheric Sounder (MAS), which flew on the space shuttle with ATMOS, the Halogen Occultation Experiment (HALOE) and Microwave Limb Sounder (MLS), which fly on the Upper Atmospheric Research Satellite (UARS), and the

Stratospheric Aerosol and Gas Experiment II (SAGE II), which flies on the Earth Radiation Budget Experiment (ERBE) satellite.

2. Comparison methodology

Ideally comparisons between instruments are performed using measurements obtained simultaneously in the same or identical air masses. Such ideal conditions are not generally achievable when comparing observations from various space-based instruments and measurements from in situ or other remote sensing instruments. Dynamical features, such as tropical and vortex filaments in extratropics/extravortex regions, can lead to ambiguity in comparisons of nearly coincident measurements, and care must be taken to compare observations made in similar air masses [Manney *et al.*, 2000, 2001]. For example, during the time period of the ATLAS-3 mission (see Table 1), the stratosphere was dynamically active where ATMOS was making measurements at low to midlatitudes in the Northern Hemisphere (NH) [Manney *et al.*, 1996]. The Arctic vortex was in an early stage of development and was responsible for drawing large tongues of tropical or subtropical air to higher latitudes [Manney *et al.*, 1999, 2000].

The gradient in water vapor mixing ratio with latitude is significant in the stratosphere [Chiou *et al.*, 1993, 1997; McCormick *et al.*, 1993; Rind *et al.*, 1993; Eluszkiewicz *et al.*, 1996, 1997; Harries *et al.*, 1996; Pan *et al.*, 1997; Rosenlof *et al.*, 1997; Nedoluha *et al.*, 1998]; thus, advection of air from the tropics to higher latitudes can lead to large variability in profiles of [H₂O] at midlatitudes. (Square brackets denote species volume mixing ratio.) Throughout this paper (i.e., for all comparisons except those with MkIV data), we have accounted for these dynamical factors by identifying comparable profiles (from data sets generally measured within a few days of one another) based on potential vorticity (PV) derived from UK Met Office- and National Centers for Environmental Prediction (NCEP)-assimilated winds. In most cases, PV was normalized by a standard value of the static stability, yielding a scaled potential vorticity (sPV) [Dunkerton and Delisi, 1986; Manney *et al.*, 1994]. For all the profiles compared here, the difference in sPV is within $4 \times 10^{-5} \text{ s}^{-1}$ and with few exceptions is within $2 \times 10^{-5} \text{ s}^{-1}$ (~20% at midlatitudes).

Most of the measurements compared were made within a week and a few degrees latitude of one another. The MkIV measurements and 1993 ER-2 observations, however, were made several weeks and/or many degrees in latitude apart from the ATMOS observations. For these comparisons, we have plotted the $[\text{H}_2\text{O}]$ measurements relative to simultaneous measurements of $[\text{N}_2\text{O}]$. We sorted the ER-2 data by PV and $[\text{N}_2\text{O}]$. Measurements made in vortex fragments were identified as having $[\text{N}_2\text{O}]$ less than 160 ppb and PV between 1.59 and $2.15 \times 10^{-5} \text{ K m}^2 \text{ kg}^{-1} \text{ s}^{-1}$. The rest of the measurements associated with PV greater than $1 \times 10^{-5} \text{ K m}^2 \text{ kg}^{-1} \text{ s}^{-1}$ (to avoid inclusion of recent tropical air masses) were characterized as having been made in extravortex air masses.

Furthermore, each CH_4 molecule oxidized in the stratosphere yields approximately two H_2O molecules [e.g., *Bates and Nicolet, 1965; Wofsy et al., 1972; Kley et al., 1979; LeTexier et al., 1988; Engel et al., 1996; Remsberg et al., 1996; Hurst et al., 1999*]. Numerous studies have shown that the sum $[\text{H}_2\text{O}] + 2[\text{CH}_4]$ is conserved (i.e., has no significant sources or sinks) throughout most of the stratosphere [e. g., *Jones et al., 1986; Abbas et al., 1996a; Engel et al., 1996; Manney et al., 1999; Zöger et al., 1999; Michelsen et al., 2000*], except in the lower winter polar vortex, where sedimentation of polar stratospheric clouds causes dehydration [e.g., *Kelly et al., 1989; Fahey et al., 1990; Rinsland et al., 1996; Hintsa et al., 1998*]. Because $[\text{H}_2\text{O}] + 2[\text{CH}_4]$ (also frequently referred to as potential water or PW) is expected to be conserved in extratropical/extravortex air masses, we have compared values of PW derived from simultaneous measurements of $[\text{CH}_4]$ and $[\text{H}_2\text{O}]$ for cases in which observations were separated by more than a week and a few degrees in latitude. We made similar comparisons with HALOE, which also measures $[\text{CH}_4]$.

When comparing data sets for which we could identify a number of similar pairs (by matching profiles with similar profiles of PV or sPV), we calculated the average fractional difference and the standard deviation of the mean difference for these pairs of profiles. The fractional difference $Diff_i$ for each pair of profiles i was given as

$$Diff_i = \frac{2[\text{H}_2\text{O}(\text{ATMOS})_i - \text{H}_2\text{O}(\text{Other})_i]}{[\text{H}_2\text{O}(\text{ATMOS})_i + \text{H}_2\text{O}(\text{Other})_i]} \quad (1)$$

The average fractional difference for N pairs of profiles was calculated as

$$\langle Diff \rangle = \frac{1}{N} \sum_1^N Diff_i, \quad (2)$$

and the standard deviation of the mean difference σ_{Diff} was calculated as

$$\sigma_{Diff} = \left[\frac{\sum_1^N (Diff_i - \langle Diff \rangle)^2}{N(N-1)} \right]^{1/2}. \quad (3)$$

3. Description of ATMOS

3.1 Instrument Description

ATMOS is a fast-response Michelson interferometer, which obtains high resolution ($\sim 0.01 \text{ cm}^{-1}$), broadband spectra through orbital sunrises and sunsets during solar occultation by the Earth. This observational technique provides immediate calibration data with each occultation, making the instrument self-calibrating and thereby eliminating long-term drift. The accuracy of such measurements is generally insensitive to changes in background transmission, e.g., resulting from heavy volcanic aerosol loading, although precision will be degraded with a significant reduction in the signal.

ATMOS is currently packaged to fly on the space shuttle. From a low-Earth orbit of $\sim 300 \text{ km}$ altitude typical of the space shuttle, an occultation observation requires $\sim 4 \text{ min}$. With an instrument scan time of 2.2 s , approximately 100 spectra are recorded, resulting in a tangent altitude spacing of $\sim 2 \text{ km}$ in the lower stratosphere to $\sim 4 \text{ km}$ in the upper stratosphere. The vertical spacing coupled with the instantaneous instrument field-of-view of $1.0\text{-}2.8 \text{ mrad}$ leads to an effective vertical resolution of $3\text{-}6 \text{ km}$ [Gunson *et al.*, 1996].

ATMOS has been deployed four times as part of the Spacelab 3 and the Atmospheric Laboratory for Applications and Science (ATLAS)-1, ATLAS-2, and ATLAS-3 missions [Kaye and Miller, 1996]. Observations from these missions cover the periods of time and ranges of latitude given in Table 1. In order to enhance the signal-to-noise ratio and minimize zero-level offsets, measurements were made in selected spectral regions defined by the optical bandpass filters listed in Table 2. For each sunrise or sunset occultation, spectra

were recorded in one of these six transmission regions; the filter selection determined which species could be retrieved for that occultation [Gunson *et al.*, 1996; Abrams *et al.*, 1996]. The systematic error of the ATMOS measurements is generally dominated by experimental uncertainty in the line strengths and the isolation of spectral features (e.g., the degree of blending or overlap with spectral features of other species), particularly at the lower tangent heights. The precision is a statistical measure of the scatter in the retrievals and is largely determined by random spectral noise, and by uncertainties in the tangent altitudes and the assumed temperature-pressure profiles.

3.2 Retrieval Description

The retrieval algorithm used for the ATMOS Version 3 (V3) data set was adapted from an algorithm developed for the analysis of MkIV balloon spectra [Toon *et al.*, in preparation]. ATMOS-V3 retrievals differ from those of Version 2 (V2) in several respects, the most noteworthy of which is the use of a simultaneous global fit for multiple species and tangent pressures, rather than a sequential onion-peeling approach for individual species [Irion *et al.*, in preparation]. These V3 profiles extend to lower altitudes and include additional species [Irion *et al.*, in preparation]. V3 retrievals in the middle stratosphere vary little from those provided by V2, but V3 retrievals in the upper and lower stratosphere and upper troposphere display less unrealistic variability and more consistency among filters than do V2 retrievals. V3 data can be obtained from <http://remus.jpl.nasa.gov/atmos/>.

For V3 water vapor, the systematic error is estimated to be $\pm 6\%$ based on uncertainties in the line strengths used in the retrievals [Brown *et al.*, 1996]. A preliminary estimate of the (1σ) random error yields an average value of 9-14% for Filters 3, 9, and 12 between 17 and 65 km with uncertainties as high as 30% in the troposphere [Michelsen *et al.*, 2000; Irion *et al.*, in preparation]. Water vapor profiles from Filters 1 and 12, which were not retrieved for V2, are available for V3, but retrievals from Filter 1 currently appear to be unreliable, perhaps because of a lack of temperature-insensitive H₂O lines for Filter 1. Retrievals of [CH₄] and [N₂O] for Filters 3, 9, and 12, which are also used in the present analysis, have an estimated systematic uncertainty of $\pm 5\%$ and precision of 5-10% between 17 and 40 km and

12-27% in the upper stratosphere and mesosphere, where abundances are smaller [*Michelsen et al.*, 2000; *Irion et al.*, in preparation]. Table 2 summarizes which species used in this analysis were retrieved with V2 and which are new retrievals for V3.

Comparisons of ATMOS-V2 measurements of $[\text{H}_2\text{O}]$ in the lower stratosphere with in situ observations from the NOAA Lyman- α hygrometer have demonstrated agreement to within $\pm 8\%$ [*Chang et al.*, 1996; *Michelsen et al.*, 1999b]. Previous analyses indicate that ATMOS-V2 is 10-15% higher than HALOE Version 17 (V17) [*Harries et al.*, 1996; *Nedoluha et al.*, 1997] and MLS prototype Version 0104 (V1014) [*Pumphrey*, 1999] in the middle and upper stratosphere. In the mesosphere ATMOS-V2 is 15-20% higher than HALOE-V17 and comparable to MLS Version 3 (V3), MAS, and the Water Vapor Millimeter-wave Spectrometer (WVMS) within the scatter of the observations [*Nedoluha et al.*, 1997]. In this paper we have made comparisons using updated versions of these data sets using ATMOS-V3, HALOE-V19, MLS-V0104, and MAS-V20.

Compared to V2 retrievals, V3 individual profiles reveal more small-scale variability (i.e., more features with a vertical scale of less than 5 km) throughout the stratosphere and display less erratic behavior in the tropopause region, thus capturing the hygropause water vapor minimum (located at or just above the tropopause) more reliably. In addition, individual occultations and the averaged profiles show a reduction for V3 by 5-10% in upper stratospheric and mesospheric water vapor. This difference is attributable to a modified selection of H_2O lines, slightly lower tangent heights above 30 km, and algorithm changes in V3 [*Irion et al.*, in preparation]. These differences bring the ATMOS observations into better agreement with HALOE, MAS, and MLS in the upper atmosphere [*Nedoluha et al.*, 1997]. With the exception of the tropopause and upper stratosphere/mesosphere regions, the average V2 and V3 stratospheric profiles are nearly identical.

4. Brief Description of Other Instruments

4.1 Lyman- α Hygrometers

The NOAA and Harvard Lyman- α hygrometers provide in situ measurements of $[\text{H}_2\text{O}]$ in the lower stratosphere from the ER-2 aircraft. Both instruments use the technique in which

H₂O is photodissociated with 121.6 nm radiation supplied by a hydrogen discharge lamp. The electronically excited OH thereby produced generates a fluorescence signal, which is proportional to the mixing ratio of H₂O. These measurements are estimated to have an accuracy of ± 5 -10% [Kelly *et al.*, 1989; Weinstock *et al.*, 1994; Hintsä *et al.*, 1999].

4.2 MkIV

The Jet Propulsion Laboratory (JPL) MkIV balloon-borne instrument is a high-resolution Fourier transform spectrometer, which is operated in a solar occultation mode. MkIV is very similar to ATMOS, and the algorithm used to retrieve the vertical mixing ratio profiles for MkIV is nearly identical to that used for the ATMOS-V3 retrievals. The accuracy for MkIV [H₂O] measurements is estimated to be 6% [Toon, 1991; Sen *et al.*, 1996; Toon *et al.*, 1999].

4.3 HALOE

HALOE is a solar occultation radiometer that was launched as part of the UARS payload in 1991. Measurements of solar absorption at 6.6 μm are used to obtain vertical profiles of [H₂O] via the ν_2 vibrational band with an estimated accuracy of 10-14% in the middle and upper stratosphere (1-10 hPa, ~ 30 -50 km), 14-19% at levels of 10-40 hPa (~ 22 -30 km), and 19-24% at 40-100 hPa (16-22 km) [SPARC, 2000]. Accuracy is estimated to be $\sim 30\%$ in the mesosphere [Harries *et al.*, 1996]. We use HALOE-V19 for the comparisons presented here.

4.4 SAGE II

SAGE II is a solar occultation radiometer that flies on ERBE. By measuring solar absorption at 940 nm, SAGE II has obtained vertical profiles of [H₂O] continuously since its deployment in 1984. At altitudes between 10 and 30 km, estimated systematic uncertainties are 20-30%, and at altitudes above and below this range, systematic error is $\sim 10\%$. Random errors are estimated to be 10-20% [Chu *et al.*, 1993; SPARC, 2000]. We use SAGE II-V6 for the comparisons presented here.

4.5 MAS

MAS is a microwave limb sounding instrument that has flown with ATMOS on the space shuttle three times as part of the ATLAS payload. MAS obtains vertical profiles of [H₂O] by measuring limb emission from the rotational transitions of H₂O at 183 GHz with a spectral

resolution of 200 kHz. Estimated retrieval errors range from 8% in the middle stratosphere to 15% in the lower stratosphere and mesosphere [Aellig *et al.*, 1996; Bevilacqua *et al.*, 1996; Hartmann *et al.*, 1996]. We use MAS-V20 for the comparisons presented here.

4.6 MLS

MLS is a microwave limb sounding instrument similar to MAS. MLS was deployed in 1991 as part of the UARS payload. Until April 1993, MLS obtained vertical profiles of [H₂O] in the stratosphere and mesosphere by recording emission from H₂O transitions at 183 GHz. Systematic uncertainties range from 8% in the middle stratosphere to 25% in the lower stratosphere and upper mesosphere [Lahoz *et al.*, 1996; Pumphrey, 1999]. We use MLS-V0104 for the comparisons presented here.

5. Comparisons

5.1 Comparisons with Lyman- α Hygrometers

The ATMOS data set from the ATLAS-3 shuttle mission offers the opportunity for comparison with measurements from the NOAA Lyman- α hygrometer. Chang *et al.* [1996] compared V2 retrievals of [H₂O] from ATMOS/ATLAS-3 with observations made by the NOAA Lyman- α hygrometer from the ER-2 during the Airborne Southern Hemisphere Ozone Experiment/Measurements for Assessing the Effects of Stratospheric Aircraft (ASHOE/MAESA) aircraft mission. This comparison demonstrated agreement to within 8% [Chang *et al.*, 1996]. Here we perform a similar analysis with V3 data.

Figure 1 shows a comparison of ATMOS/ATLAS-3 data with near coincident in situ data from the NOAA Lyman- α hygrometer. Figures 1a and 1b show individual ATMOS occultations compared with portions of two ER-2 flights. The ER-2 data were averaged in 10-K potential temperature segments of up to 1000 points, and the error bars represent the 1σ standard deviation of the data. Figures 1c and 1d show the fractional differences between the measurements from the two instruments. As a result of the transport processes described in Section 2, ATMOS and the ER-2 sampled air originally from different regions within the same latitude band and pressure bin. We have attempted to account for dynamical variability by sorting the data based on PV derived from Met Office-assimilated winds, and Figures 1e

and 1f show the differences between the PV profiles corresponding to the ER-2 and ATMOS measurements.

The data in Figure 1a represent midlatitude (extravortex/extratropical) profiles. For these profiles, the differences between the mean values of the NOAA Lyman- α hygrometer and the ATMOS-V3 data are less than 10%; the ATMOS values are on average \sim 5% lower than those from the NOAA instrument.

Data in Figure 1b are associated with tropical air. The tropical profiles demonstrate oscillations in $[\text{H}_2\text{O}]$ characteristic of the water vapor seasonal cycle. That is, the abundance of H_2O in the tropical lower stratosphere has been observed to be correlated with mean tropical tropopause temperatures, which undergo an annual cycle [Newell and Gould-Stewart, 1981; Jones *et al.*, 1986; McCormick *et al.*, 1993; Rind *et al.*, 1993; Rosenlof *et al.*, 1997]. During NH winter, tropopause temperatures are the lowest, and $[\text{H}_2\text{O}]$ at the tropical tropopause is at a minimum; during the NH summer tropical tropopause temperatures and $[\text{H}_2\text{O}]$ are at a maximum. As air masses ascend in the tropical stratosphere, this oscillation in $[\text{H}_2\text{O}]$ is maintained, leading to oscillations in the vertical profile of $[\text{H}_2\text{O}]$ in the tropics [e.g., McCormick *et al.*, 1993; Mote *et al.*, 1995, 1996; Abbas *et al.*, 1996b; Randel *et al.*, 1998, 2001; Michelsen *et al.*, 2000], as shown in Figure 1b. The amplitude is larger for the in situ observations because of their higher vertical resolution, but the ATMOS measurements at least partially capture the seasonal cycle. The large variability in the fractional differences for the tropics largely results from this limited ability of the ATMOS instrument to measure the sharp oscillations associated with the lower stratospheric seasonal cycle.

During the ATLAS-2 mission (April 8-16, 1993), ATMOS made measurements in regions inside and outside the springtime Arctic vortex. Just following this mission, the NOAA and Harvard Lyman- α hygrometers flew at northern middle and high latitudes aboard the ER-2 as part of the Stratospheric Photochemistry, Aerosols, and Dynamics Expedition (SPADE) aircraft campaign (April 23-May 18). During SPADE the ER-2 encountered large fragments of the Arctic vortex, which broke up between the ATLAS-2 and SPADE missions (April 20). A previous comparison of ATMOS-V2 retrievals of H_2O from ATLAS-2 and

measurements of H_2O from the NOAA Lyman- α hygrometer made during SPADE demonstrated good agreement, as long as the distinction between vortex and extravortex air masses was taken into account [Michelsen *et al.*, 1999b]. This distinction was accounted for by sorting the in situ data based on the relative abundances of long-lived tracers, one of which was H_2O . For the present study we have re-sorted the data based on PV and $[\text{N}_2\text{O}]$ (see Section 2).

Figure 2 shows averages of ATMOS-V3 observations from inside and outside the vortex with error bars representing the weighted standard deviation of the mean. These averages are compared with averages of measurements made by the NOAA and Harvard Lyman- α hygrometers inside and outside vortex fragments on April 30 and May 3, 6, and 7. Data from the flight on April 23 were excluded because of a problem with the inlet of the Harvard instrument during that flight. The in situ observations were averaged relative to $[\text{N}_2\text{O}]$ provided by the Aircraft Laser Infrared Absorption Spectrometer (ALIAS) [Webster *et al.*, 1994] in 10-ppb segments, and error bars represent one standard deviation of the data. The fractional differences between the ATMOS and Lyman- α hygrometer measurements are plotted in the bottom panels of Figure 2. ATMOS measurements are 0-5% higher than those provided by the NOAA instrument and systematically 10-16% lower than those made by the Harvard instrument for this data set.

During SPADE, ALIAS made measurements of $[\text{CH}_4]$ with an estimated (1σ) accuracy of 5% [Webster *et al.*, 1994]. Observations of $[\text{CH}_4]$ from this instrument have been shown to be consistent with ATMOS-V3 observations to within 5% [Michelsen *et al.*, 1999c]. We have derived potential water for the flights used in Figure 2 by combining ALIAS $[\text{CH}_4]$ measurements with simultaneous measurements of $[\text{H}_2\text{O}]$ from the NOAA and Harvard Lyman- α hygrometers and compared the results with PW derived for the corresponding ATMOS occultations. Figure 3 shows that values of PW based on ATMOS data are 0-5% higher than those derived from NOAA Lyman- α hygrometer data and 5-11% lower than values derived from Harvard Lyman- α hygrometer data. The agreement between ATMOS

and ALIAS [CH₄] is good, and these differences in PW are thus predominantly due to differences between [H₂O] measurements.

The only significant source of stratospheric PW is influx of tropospheric air, and the only substantial stratospheric sink of PW is polar vortex dehydration via sedimentation of polar stratospheric clouds. PW is thus generally conserved in extravortex/extratropical regions, as shown in Figures 3b and 3e by the approximately constant value (within experimental uncertainty) outside the vortex. Stratospheric PW has been observed to be increasing with time, however, at an average rate of ~ 0.065 ppm/yr [Engel *et al.*, 1996; Evans *et al.*, 1998; Nedoluha *et al.*, 1998; Randel *et al.*, 1999; Michelsen *et al.*, 2000]. This increase in PW is predominantly attributable to an increase in stratospheric humidity [Oltmans and Hoffman, 1995; Engel *et al.*, 1996; Evans *et al.*, 1998; Nedoluha *et al.*, 1998; Johnson *et al.*, 1999; Randel *et al.*, 1999; Michelsen *et al.*, 2000; Oltmans *et al.*, 2000; Smith *et al.*, 2000; SPARC, 2000; Rosenlof *et al.*, 2001]. Hurst *et al.* [1999], however, inferred a slightly negative but statistically insignificant trend in lower stratospheric PW and [H₂O], although the time period for which this analysis was performed (early 1993 to late 1997) was comparable in duration and overlapped significantly with many of the other studies [see Plate 1 in Michelsen *et al.*, 2000]. One explanation for the small trend and large uncertainty yielded by the analysis of Hurst *et al.* [1999] is that the study focuses on the lower stratosphere, where water vapor trends are more difficult to assess, possibly because of more rapid mixing between tropical and extratropical air masses at these altitudes.

Assuming that the average stratospheric age of Arctic vortex air is 3.1-7.5 years older than that of extravortex air [Pollock *et al.*, 1992; Harnisch *et al.*, 1996], the positive trend in PW would lead to higher PW by 0.2-0.5 ppm outside than inside the vortex in the absence of dehydration. This range of values is consistent with the average differences between lower stratospheric extravortex (Figure 3b) and vortex (Figure 3a) observations of 0.4 ± 0.6 ppm for ATMOS and 0.249 ± 0.006 ppm for the NOAA Lyman- α hygrometer. The difference of -0.031 ± 0.006 ppm between extravortex (Figure 3e) and vortex (Figure 3d) values of PW inferred from the Harvard Lyman- α hygrometer would imply a negative trend in PW, which

is more consistent with the results of *Hurst et al.* [1999]. For the in situ data, the extravortex averages included points for which $[\text{N}_2\text{O}]$ was between 200 and 250 ppb. The difference in PW between extravortex and vortex air inferred from ATMOS-V3 data is smaller than the ~ 0.7 ppm difference noted in a previous analysis based on ATMOS-V2 data [*Michelsen et al.*, 1999b]. Dehydration could additionally contribute to these differences, but denitrification usually accompanies dehydration, and strong evidence of denitrification was not apparent in Arctic vortex air masses during this time period [*Manney et al.*, 1999; *Michelsen et al.*, 1999b].

An additional loss mechanism for upper atmospheric H_2O is photolysis in the middle and upper mesosphere ($>\sim 60$ km). As suggested by *Michelsen et al.* [1999b], the deficit in PW could thus alternatively be explained by air descended from these altitudes inside the vortex. Observations made by *Ray et al.* [Descent and mixing in the 1999-2000 northern polar vortex inferred from in situ measurements, submitted to *J. Geophys. Res.*] showed evidence of descended mesospheric air enhanced in H_2 resulting from H_2O photolysis inside the Arctic vortex at altitudes of 25-35 km during spring 2000. Tracer distributions in the region of the vortex where the deficit in PW was observed (17-20 km), however, appear to be inconsistent with air originating from altitudes above ~ 50 km [*Michelsen et al.*, 1998]. Furthermore, the PW deficit appears at altitudes below the region (22-25 km) in which elevated abundances of CO observed during this time period suggest descent from altitudes above 45 km [*Rinsland et al.*, 1999].

5.2 Comparisons with MkIV

Comparisons between ATMOS and MkIV data collected in similar air masses are shown in Figure 4. Figure 4a shows the mean of ATMOS-V3 data collected at midlatitudes during fall in the Southern Hemisphere (SH) from ATLAS-1 compared with MkIV observations from midlatitudes made 6 months later during fall in the NH. Figure 4b shows a comparison of the mean of ATMOS/ATLAS-2 extravortex observations with data from a MkIV flight made 1-2 weeks earlier at northern midlatitudes. Figure 4c shows data from northern midlatitudes during fall for MkIV (1993) and ATMOS/ATLAS-3 (1994). The comparisons

are summarized in Figure 4d, which shows that the ATMOS and MkIV measurements of [H₂O] differ by less than 5% below 6 hPa (35 km) and by less than 2% between 47 and 10 hPa (21-31 km) under similar atmospheric conditions.

MkIV measures [CH₄] with an accuracy (1σ) of 5% [Toon *et al.*, 1999], and a comparison of PW from MkIV and ATMOS for the cases discussed above is shown in Figures 4e-h. For these cases, the agreement between the corresponding MkIV and ATMOS values of PW is within 4% below 35 km (within 2% between 21 and 31 km).

For Figure 5 scaled PV derived from Met Office-assimilated winds [Manney *et al.*, 1994] was used to identify profiles recorded in similar air masses. This figure shows a comparison of profiles of [H₂O] (Figures 5a and c) and PW (Figures 5b and d) from April 1993. Differences between the [H₂O] profiles are within 5% except at altitudes above ~18 hPa (27 km) and at a level near ~35 hPa (23 km). The differences between the PW profiles demonstrate much better agreement at these levels, suggesting that the larger discrepancies apparent for [H₂O] are attributable to atmospheric variability.

The level of agreement demonstrated here between MkIV and ATMOS is not surprising given the similarity of the MkIV and ATMOS instruments and their data reduction methods. This comparison is thus a good test of the selection criteria used for these comparisons and demonstrates the success of the comparison methodology, particularly given that the data shown in Figure 5 were separated by many more degrees of latitude than any of the data sets used in the other comparisons presented.

5.3 Comparisons with HALOE

Figure 6 shows comparisons between averaged and individual ATMOS and HALOE profiles made during ATLAS-3. All of the ATMOS profiles and all but the tropical HALOE profile are from sunset occultations. The fractional differences are shown in Figures 6e-h. Profiles from similar air masses were identified based on sPV, and differences in sPV between the profiles compared are shown in Figures 6i-l. Each ATMOS profile used in the average was paired with a HALOE profile with comparable sPV. The data in Figure 6b were obtained inside the developing vortex (protovortex). The data in Figure 6c are more

characteristic of midlatitude (extravortex/extratropical) air, and the data in Figure 6d are associated with tropical air.

Shapes of the profiles in Figures 6a-d agree well, and there is good agreement in the vertical registration of these profiles. The average fractional differences between the ATMOS and HALOE observations shown in Figure 6e suggest that the differences between these instruments are generally less than 10% and are of order 5% (ATMOS larger) between 70 and 1 hPa (18 and 50 km). The standard deviation of the mean difference encompasses zero in the middle stratosphere, indicating that the systematic differences near 40 km are not statistically significant. Greater differences (as much as 63%) are observed in the upper mesosphere (>70 km). At these altitudes, however, water vapor abundances are smaller (i.e., small absolute differences in retrieved mixing ratio may lead to large fractional differences), and PV is not available for matching profiles (i.e., comparisons are less reliable). The agreement observed for the stratosphere appears to be better than that demonstrated in a previous comparison of ATMOS-V2 data with HALOE-V17 observations, which showed that the ATMOS values were systematically higher than those from HALOE in the middle stratosphere by 10-15% [Harries *et al.*, 1996]. In addition, there appears to be no evidence in either the HALOE or ATMOS profiles of an unexplained enhancement in mesospheric water vapor that was observed in HALOE-V17 profiles [Siskind and Summers, 1998].

The variability in the individual profile comparisons can partially be explained by atmospheric variability, despite the generally successful attempt to match profiles using sPV. Manney *et al.* [2000] have shown that the ATMOS profiles used to represent the protovortex (ss40) and midlatitude (ss64) regions were perturbed by filaments from outside these regions and that the low resolution PV used here to match profiles did not consistently capture the signatures of these filaments. For example, at ~2 hPa (41.5 km, 1430 K) the ATMOS protovortex profile passes through a filament from the edge of the protovortex, and at ~15 hPa (28 km, 700 K) this profile includes a filament that originated at lower latitudes [Manney *et al.*, 2000]. The ATMOS midlatitude profile passes through several filaments from the protovortex edge at ~20 hPa (27 km, 670 K), ~15 hPa (28.5 km, 730 K), and ~3.8 hPa (37.5

km, 1170 K) and a filament from low latitudes at ~ 45 hPa (21.5 km, 514 K). *Manney et al.* [2001] used the same ATMOS and HALOE occultations for a comparison of $[\text{O}_3]$; their analysis suggests that the HALOE occultations probably did not encounter most of these filaments.

Comparing profiles for PW should compensate for some of this variability. Since CH_4 is oxidized in the stratosphere to form H_2O , $[\text{CH}_4]$ and $[\text{H}_2\text{O}]$ are expected to be anti-correlated. At several of the levels where ATMOS $[\text{H}_2\text{O}]$ is low (high) relative to HALOE values, ATMOS $[\text{CH}_4]$ is higher (lower) than the HALOE values (see Figures 7j and k). Figures 7a-d show the comparison of PW corresponding to the profiles compared in Figures 6a-d, and Figures 7e-h show the fractional differences for PW (solid) and $[\text{H}_2\text{O}]$ (dashed). At most levels the solid and dashed lines in Figures 7e-h are indistinguishable, demonstrating good agreement between ATMOS and HALOE $[\text{CH}_4]$. At several levels, where ATMOS encountered a filament and HALOE did not, the fractional differences are smaller for PW than for $[\text{H}_2\text{O}]$, confirming that these differences are at least partially attributable to atmospheric variability. In fact, the fractional differences shown in Figure 7e are smaller at each stratospheric level where the mean differences shown in Figure 6e appeared to be statistically significant. The comparison of PW from the averages thus suggests that the differences between HALOE and ATMOS in the lower stratosphere shown in Figure 6e are probably due to differences in the mean age of air used in the averages and that the HALOE average includes air that is younger than that used in the ATMOS average. This result indicates that the level of agreement between HALOE and ATMOS is within 8% throughout the stratosphere.

5.4 Comparisons with SAGE II

Figure 8 shows the same average and individual ATMOS profiles as shown in Figure 6 compared with SAGE II profiles with similar sPV. All profiles compared are from sunset occultations. The fractional differences are shown in Figures 8e-h, and the differences in the corresponding sPV are shown in Figures 8i-l. Agreement between the two instruments is very good (within 5%) between 15 and 3.8 hPa (28-38 km), despite large variability in

differences between individual profiles. In the lower stratosphere ATMOS [H₂O] is systematically higher than that of SAGE II by as much as 41%. A high bias relative to SAGE II [H₂O] in the lower stratosphere is consistent with previous comparisons of SAGE II-V6 retrievals with frostpoint hygrometer and other satellite measurements [*Chiou et al.*, 2000; *SPARC*, 2000].

Figure 9 shows a comparison of profiles from 1985, i.e., prior to the Pinatubo eruption. The Spacelab 3 mission did not produce many profiles. For this comparison we used National Center for Atmospheric Research (NCAR)/NCEP reanalysis assimilation data [*Kalnay et al.*, 1996]. The averages shown in Figure 9a include 6 sunset profiles from the subtropics. Two of these profiles are shown separately in Figures 9b and 9c. These comparisons indicate agreement to within 17% between 38 and 3.2 hPa (23-39 km), but demonstrate much larger systematic differences in the lower stratosphere. In contrast to the post-Pinatubo comparison, ATMOS is systematically lower than SAGE II in the lower stratosphere, particularly near 70 hPa, i.e., just above the tropopause, where the SAGE II profiles have a sharp maximum. The SAGE II sunset occultations from this time period consistently show this feature at all latitudes, suggesting that it is not attributable to low-latitude atmospheric variability. The sunrise occultations, on the other hand, do not include this feature and appear to give better agreement in the lower stratosphere with the ATMOS profiles, as shown in Figure 9d. The number of ATMOS profiles available for the sunrise comparisons is limited to two, however, one of which does not extend below 68 hPa. A comparison of SAGE II sunrise and sunset [H₂O] profiles from the same latitude region (19-22°S) and time period (May 6-7, 1985) shows differences of 10-22% between 68 and 18 hPa (~19-27 km). Some of the differences observed in these comparisons may be caused by interference of aerosol loading in the lower stratosphere. By spring 1985, the lower stratosphere had not fully recovered from the 1982 eruption of El Chichón. Below 24 km aerosol extinction at 1 micrometer exceeded the value of 1×10^{-4} recommended by *Rind et al.* [1993] as the maximum value at which the SAGE II [H₂O] measurements should be considered reliable.

5.5 Comparisons with MAS

Figure 10 shows comparisons between averaged and individual ATMOS and MAS profiles from the ATLAS-3 mission. Fractional differences between profiles are shown in Figures 10e-h, and differences in sPV between the profiles compared are shown in Figures 10i-l. The individual ATMOS profiles and the profiles used in the average are the same as those used in the comparison with HALOE shown in Figure 6 and with SAGE II shown in Figure 8. The comparisons of the individual profiles (Figures 10b-d) suggest that the ATMOS data have a wet bias in the mesosphere relative to MAS, but the averaged profiles (Figure 10a) and the large standard deviation of the mean difference (Figure 10e), which encompasses zero, indicate that this difference is not statistically significant. The agreement between ATMOS and MAS is generally within 7% between 12 and 0.8 hPa (30-50 km) but with large variability. ATMOS tends to be higher in the lower stratosphere, where average differences are closer to 13%. As with the comparison with HALOE, differences in the individual profiles appear to be largest at levels where ATMOS encountered filaments from different regions and where MAS apparently did not encounter such filaments [*Manney et al.*, 2001]. Furthermore, because the vertical resolution of MAS (~7 km) is much lower than that of ATMOS, if MAS did encounter one of these filaments, the comparison may not show good agreement.

5.6 Comparisons with MLS

Figure 11 shows a comparison of ATMOS-V3 data with MLS-V0104 [*Pumphrey, 1999*] observations from southern latitudes during spring 1992 and 1993. Unweighted mean values are shown for 10 pairs of profiles recorded at southern midlatitudes in March 1992 (Figure 11a), and individual profile comparisons are made with observations from inside (Figure 11c) and outside (Figure 11b) the protovortex in 1992 and outside the protovortex in 1993 (Figure 11d). Fractional differences between the profiles are shown in Figures 11e-h. The data were sorted, as above, based on sPV, and differences between the sPV profiles are shown in Figures 11i-l. The ATMOS data tend to exceed the MLS measurements in the middle and upper stratosphere. The difference is ~0.6 ppm and corresponds to an average fractional

difference of <14% throughout most of the stratosphere. The offset decreases in the mesosphere. Throughout most of the stratosphere and mesosphere, the standard deviation of the mean fractional differences does not approach the zero crossing line (Figure 11e), indicating that this difference is statistically significant. These differences are consistent with a recent comparison of MLS-V0104 with ATMOS-V2 water vapor observations [Pumphrey, 1999].

6. Summary and Conclusions

Because atmospheric water vapor abundance varies with altitude, latitude, and frequently longitude, the success of comparisons of [H₂O] measurements by instruments on different platforms depends on the reliability with which measurement conditions can be matched. We have used PV to pair profiles obtained within 6 days and 9 degrees of latitude of one another. We have also shown that measurements of [H₂O] made several weeks and many degrees of latitude apart can be compared relative to simultaneously measured [N₂O]. In addition, we have used simultaneously measured [CH₄] to identify and limit differences attributable to atmospheric variability related to different stratospheric ages of air masses.

Results of the comparisons are summarized for different altitude ranges in Table 3 and Figure 12. ATMOS tends to be biased high relative to most of the instruments, but is usually within their respective experimental uncertainties. In the middle stratosphere ATMOS-V3 demonstrates agreement to within 15% with the 5 instruments that make measurements in this region of the atmosphere. Agreement is within 18% throughout the stratosphere with all of the instruments with the exception of SAGE II. Agreement deteriorates in the upper mesosphere, where [H₂O] is lower and small differences in mixing ratio lead to large fractional differences and where PV, and thus a good way of matching profiles, is not available. Agreement also deceptively suffers when the low resolution PV used to sort the data fails to identify filaments from other types of air masses included in one but not the other of the profiles in a comparison. In addition, since the vertical resolution of the ATMOS instrument is limited (3-6 km), oscillations with a characteristic wavelength of less than a few km (e.g., the seasonal cycle in [H₂O] observed in the tropics and subtropics) are not well

resolved by ATMOS. Thus, under conditions when the water vapor seasonal cycle is large, ATMOS does not agree well with the in situ observations, which have a much higher spatial resolution.

In the lower stratosphere, for the cases presented here, ATMOS-V3 water vapor observations are 0-5% higher than measurements from the NOAA Lyman- α hygrometer and 10-16% lower than those from the Harvard Lyman- α hygrometer for comparisons with measurements made in April and May 1993. ATMOS measurements are ~5% lower than those from the NOAA instrument from November 1994. Agreement between ATMOS and MkIV is within 5% below 35 km and within 2% between 21 and 31 km. ATMOS measurements are generally higher than, but within 8% of, HALOE measurements throughout the stratosphere. ATMOS values are also typically higher than, but within 7% of, MAS values between 30 and 50 km and are ~13% higher than MAS values in the lower stratosphere. ATMOS observations are ~0.6 ppm (7-14%) higher than those of MLS-V0104 in the middle and upper stratosphere. This offset is not as large in the lower stratosphere and mesosphere, but the percent difference is comparable. Mean differences between ATMOS and SAGE II are within 5% between 28 and 38 km, but ATMOS values are as much as 41% higher than those from SAGE II in the lower stratosphere for the comparison of data from November 1994. In contrast, ATMOS appears to be as much as 59% lower than SAGE II at altitudes just above the tropopause for the comparison of sunset data from April/May 1985. SAGE II sunrise occultations from this time period appear to give better agreement with ATMOS in the lower stratosphere. These differences between SAGE II and ATMOS are probably partially attributable to interferences in the SAGE II retrievals from enhanced loading of lower stratospheric aerosols from the eruption of El Chichón in 1982.

With the exception of SAGE II, agreement among the instruments compared here is generally within 15% in the middle to lower stratosphere and mesosphere and within 10% in the middle to upper stratosphere. At altitudes near 30 km, all measurements, including those of SAGE II, agree to within 10%. Analyses of trends apparent in data sets from individual instruments have suggested that stratospheric water vapor is increasing at a rate of ~1%/yr

[Oltmans and Hoffman, 1995; Evans et al., 1998; Nedoluha et al., 1998; Randel et al., 1999; Michelsen et al., 2000; Oltmans et al., 2000; Smith et al., 2000; Rosenlof et al., 2001; SPARC, 2000]. Although the present level of agreement among different instruments (~10%) is very good considering the diversity of measurement techniques, it is inadequate for resolving the trend in stratospheric water vapor using combined data sets [Rosenlof et al., 2001; SPARC, 2000].

Acknowledgments. We thank J. R. Holton and K. H. Rosenlof for initiating our involvement in the SPARC water vapor assessment, which motivated much of the work presented in this paper, D. G. Johnson for enlightening discussions, and P. A. Newman for PV associated with the ER-2 observations. We thank the NASA Langley Research Center (NASA-LaRC) and the NASA Langley Radiation and Aerosols Branch for supplying the SAGE II V6 data. This work was supported by the National Aeronautics and Space Administration (NASA) Atmospheric Chemistry Modeling and Analysis Program and the SAGE III instrument team. Research at JPL, California Institute of Technology, was performed under contract to NASA. Contribution from the Univ. of Liège was supported by OSTC, Brussels.

References

- Abbas, M. M., et al., The hydrogen budget of the stratosphere inferred from ATMOS measurements of H₂O and CH₄, *Geophys. Res. Lett.*, *23*, 2405-2408, 1996a.
- Abbas, M. M., et al., Seasonal variations of water vapor in the lower stratosphere inferred from ATMOS/ATLAS-3 measurements of H₂O and CH₄, *Geophys. Res. Lett.*, *23*, 2401-2404, 1996b.
- Abrams, M. C., A. Y. Chang, M. R. Gunson, M. M. Abbas, A. Goldman, F. W. Irion, H. A. Michelsen, M. J. Newchurch, C. P. Rinsland, G. P. Stiller, and R. Zander, On the assessment and uncertainty of atmospheric trace gas burden measurements with high resolution infrared solar occultation spectra from space by the ATMOS experiment, *Geophys. Res. Lett.*, *23*, 2337-2340, 1996.

- Aellig, C. P., J. Bacmeister, R. M. Bevilacqua, M. Daehler, D. Kriebel, T. Pauls, D. Siskind, N. Kämpfer, J. Langren, G. Hartmann, A. Berg, J. H. Park, and J. M. Russell III, Spaceborne H₂O observations in the Arctic stratosphere and mesosphere in the spring of 1992, *Geophys. Res. Lett.*, *23*, 2325-2328, 1996.
- Bates, D. R., and M. Nicolet, The photochemistry of atmospheric water vapor, *J. Geophys. Res.*, *55*, 301-327, 1950.
- Bevilacqua, R. M., D. Kriebel, T. Pauls, C. Aellig, D. E. Siskind, M. Daehler, J. J. Olivero, S. E. Puliafito, G. K. Hartmann, N. Kämpfer, A. Berg, and C. L. Croskey, MAS measurements of the latitudinal distribution of water vapor and ozone in the mesosphere and lower thermosphere, *Geophys. Res. Lett.*, *23*, 2317-2320, 1996.
- Brown, L. R., M. R. Gunson, R. A. Toth, F. W. Irion, C. P. Rinsland, and A. Goldman, The 1995 Atmospheric Trace Molecule Spectroscopy (ATMOS) line list, *Appl. Opt.*, *35*, 2828-2848, 1996.
- Chang, A. Y., R. J. Salawitch, H. A. Michelsen, M. R. Gunson, M. C. Abrams, R. Zander, C. P. Rinsland, M. Loewenstein, J. R. Podolske, M. H. Proffitt, J. J. Margitan, D. W. Fahey, R.-S. Gao, K. K. Kelly, J. W. Elkins, C. R. Webster, R. D. May, K. R. Chan, M. M. Abbas, A. Goldman, F. W. Irion, G. L. Manney, M. J. Newchurch, and G. P. Stiller, A comparison of measurements from ATMOS and instruments aboard the ER-2 aircraft: Tracers of atmospheric transport, *Geophys. Res. Lett.*, *23*, 2389-2392, 1996.
- Chiou, E. W., M. P. McCormick, L. R. McMaster, W. P. Chu, J. C. Larsen, D. Rind, and S. Oltmans, Intercomparison of stratospheric water vapor observed by satellite experiments: Stratospheric Aerosol and Gas Experiment II versus Limb Infrared Monitor of the Stratosphere, and Atmospheric Trace Molecule Spectroscopy, *J. Geophys. Res.*, *98*, 4875-4887, 1993.
- Chiou, E. W., M. P. McCormick, and W. P. Chu, Global water vapor distributions in the stratosphere and upper troposphere derived from 5.5 years of SAGE II observations (1986-1991), *J. Geophys. Res.*, *102*, 19,105-19,118, 1997.

- Chiou, E. W., L. Thomason, and S. Burton, Assessment of the version 6 SAGE II water vapor data set (abstract), Proceedings of the Quadrennial Ozone Symposium, Sapporo, July 3-8, 2000.
- Chu, W. P., E. W. Chiou, J. C. Larsen, L. W. Thomason, D. Rind, J. J. Buglia, S. Oltmans, M. P. McCormick, and L. M. McMaster, Algorithms and sensitivity analyses for stratospheric aerosol and gas experiment II water vapor retrieval, *J. Geophys. Res.*, *98*, 4857-4866, 1993.
- Dunkerton, T. J., and D. P. Delisi, Evolution of potential vorticity in the winter stratosphere of January-February, 1979, *J. Geophys. Res.*, *91*, 1199-1208, 1986.
- Dvortsov, V. L., and S. Solomon, Response of the stratospheric temperatures and ozone to past and future increases in stratospheric humidity, *J. Geophys. Res.*, *106*, 7505-7514, 2001.
- Eluszkiewicz, J., D. Crisp, R. Zurek, L. Elson, E. Fishbein, L. Froidevaux, J. Waters, R. G. Grainger, A. Lambert, R. Harwood, and G. Peckham, Residual circulation in the stratosphere and lower mesosphere as diagnosed from Microwave Limb Sounder data, *J. Atmos. Sci.*, *53*, 217-240, 1996.
- Eluszkiewicz, J., D. Crisp, R. G. Grainger, A. Lambert, A. E. Roche, J. B. Kumer, and J. L. Mergenthaler, Sensitivity of the Residual circulation diagnosed from the UARS data to the uncertainties in the input fields and to the inclusion of aerosols, *J. Atmos. Sci.*, *54*, 1739-1757, 1997.
- Engel, A., C. Schiller, U. Schmidt, R. Borchers, H. Ovarlez, and J. Ovarlez, The total hydrogen budget in the Arctic winter stratosphere during the European Arctic Stratospheric Ozone Experiment, *J. Geophys. Res.*, *101*, 14,495-14,503, 1996.
- Evans, S. J., R. Toumi, J. E. Harries, M. P. Chipperfield, and J. M. Russell III, Trends in stratospheric humidity and the sensitivity of ozone to these trends, *J. Geophys. Res.*, *103*, 8715-8725, 1998.
- Fahey, D. W., et al., Observations of denitrification and dehydration in the winter polar stratospheres, *J. Geophys. Res.*, *344*, 321-324, 1990.

- Farmer, C. B., O. F. Raper, and F. G. O'Callaghan, Final report on the first flight of the ATMOS instrument during the Spacelab 3 mission, April 29 through May 6, 1985, *JPL Publication 87-32*, 1987.
- Forster, P. M. de F., and K. P. Shine, Stratospheric water vapour changes as a possible contributor to observed stratospheric cooling, *Geophys. Res. Lett.*, *26*, 3309-3312, 1999.
- Gunson, M. R., C. B. Farmer, R. H. Norton, R. Zander, C. P. Rinsland, J. H. Shaw, and B.-C. Gao. Measurements of CH₄, N₂O, CO, H₂O, and O₃ in the middle atmosphere by the Atmospheric Trace Molecule Spectroscopy Experiment on Spacelab 3, *J. Geophys. Res.*, *95*, 13,867-13,882, 1990.
- Gunson, M. R., M. M. Abbas, M. C. Abrams, M. Allen, L. R. Brown, T. L. Brown, A. Y. Chang, A. Goldman, F. W. Irion, L. L. Lowes, E. Mahieu, G. L. Manney, H. A. Michelsen, M. J. Newchurch, C. P. Rinsland, R. J. Salawitch, G. P. Stiller, G. C. Toon, Y. L. Yung, and R. Zander, The Atmospheric Trace Molecule Spectroscopy (ATMOS) experiment: Deployment on the ATLAS Space Shuttle missions, *Geophys. Res. Lett.*, *23*, 2333-2336, 1996.
- Harnisch, J., R. Borchers, P. Fabian, and M. Maiss, Tropospheric trends of CF₄ and C₂F₆ since 1982 derived from SF₆ dated stratospheric air, *Geophys. Res. Lett.*, *23*, 1099-1102, 1996.
- Harries, J. E., J. M. Russell III, A. F. Tuck, L. L. Gordley, P. Purcell, K. Stone, R. M. Bevilacqua, M. R. Gunson, G. Nedoluha, and W. A. Traub, Validation of measurements of water vapor from the Halogen Occultation Experiment (HALOE), *J. Geophys. Res.*, *101*, 10,205-10,216, 1996.
- Hartmann, G. K., R. M. Bevilacqua, R. M., P. R. Schwartz, N. Kämpfer, K. F. Künzi, C. P. Aellig, A. Berg, W. Boogaerts, B. J. Connor, C. L. Croskey, M. Daehler, W. Degenhardt, H. D. Dicken, D. Goldizen, D. Kriebel, J. Langen, A. Loidl, J. J. Olivero, T. A. Pauls, S. E. Puliafito, M. L. Richards, C. Rudin, J. J. Tsou, W. B. Waltman, G. Umlauf, and R. Zwick, Measurements of O₃, H₂O, and ClO in the middle atmosphere using the millimeter-wave atmospheric sounder (MAS), *Geophys. Res. Lett.*, *23*, 2313-2316, 1996.

- Hints, E. J., et al., Dehydration and denitrification in the Arctic polar vortex during the 1995-1996 winter, *Geophys. Res. Lett.*, *25*, 501-504, 1998.
- Hints, E. J., E. M. Weinstock, J. G. Anderson, R. D. May, and D. F. Hurst, On the accuracy of in situ water vapor measurements in the troposphere and lower stratosphere with the Harvard Lyman- α hygrometer, *J. Geophys. Res.*, *104*, 8183-8189, 1999.
- Hofmann, D. J., and S. J. Oltmans, The effect of stratospheric water vapor on the heterogeneous reaction rate of ClONO₂ and H₂O, *Geophys. Res. Lett.*, *19*, 2211-2214, 1992.
- Hurst, D. F., G. S. Dutton, P. A. Romashkin, P. R. Wamsley, F. L. Moore, J. W. Elkins, E. J. Hints, E. M. Weinstock, R. L. Herman, E. J. Moyer, D. C. Scott, R. D. May, and C. R. Webster, Closure of the total hydrogen budget of the northern extratropical lower stratosphere, *J. Geophys. Res.*, *104*, 8191-8200, 1999.
- Johnson, D. G., K. W. Jucks, W. A. Traub, K. V. Chance, G. C. Toon, J. M. Russell III, and M. P. McCormick, Stratospheric age spectra derived from observations of water vapor and methane, *J. Geophys. Res.*, *104*, 21,595-21,602, 1999.
- Jones, R. L., J. A. Pyle, J. E. Harries, A. M. Zavody, J. M. Russell III, and J. C. Gille, The water vapour budget of the stratosphere studied using LIMS and SAMS satellite data, *Q. J. R. Meteor. Soc.*, *112*, 1127-1143, 1986.
- Kalnay, E., M. Kanamitsu, R. Kistler, W. Collins, D. Deaven, L. Gandin, M. Iredell, S. Saha, G. White, J. Woollen, Y. Zhu, M. Chelliah, W. Ebisuzaki, W. Higgins, J. Janowiak, M. C. Ko, C. Ropelewski, J. Wang, A. Leetmaa, R. Reynolds, R. Jenne, and D. Joseph, The NCAR/NCEP 40-year reanalysis project, *Bull. Am. Meteorol. Soc.*, *77*, 437-471, 1996.
- Kaye, J. A., and T. L. Miller, The ATLAS series of shuttle missions, *Geophys. Res. Lett.*, *23*, 2285-2288, 1996.
- Kelly, K. K., A. F. Tuck, D. M. Murphy, M. H. Proffitt, D. W. Fahey, R. L. Jones, D. S. McKenna, M. Loewenstein, J. R. Podolske, S. E. Strahan, G. V. Ferry, K. R. Chan, J. F. Vedder, G. L. Gregory, W. D. Hypes, M. P. McCormick, E. V. Browell, and L. E. Heidt,

- Dehydration in the lower Antarctic stratosphere during late winter and early spring, 1987, *J. Geophys. Res.*, *94*, 11,317-11,357, 1989.
- Kley, D., E. J. Stone, W. R. Henderson, J. W. Drummond, W. J. Harrop, A. L. Schmeltekopf, T. L. Thomson, and R. H. Winkler, In situ measurements of the mixing ratio of water vapor in the stratosphere, *J. Atmos. Sci.*, *36*, 2513-2524, 1979.
- Lahoz, W. A., M. R. Suttie, L. Froidevaux, R. S. Harwood, C. L. Lau, T. A. Lungu, G. E. Peckham, H. C. Pumphrey, W. G. Read, Z Shippony, R. A. Suttie, J. W. Waters, G. E. Nedoluha, S. J. Oltmans, J. M. Russell III, and W. A. Traub, Validation of UARS microwave limb sounder 183 GHz H₂O measurements, *J. Geophys. Res.*, *101*, 10,129-10,149, 1996.
- LeTexier, H., S. Solomon, and R. R. Garcia, The role of molecular hydrogen and methane oxidation in the water vapor budget of the stratosphere, *Q. J. R. Meteorol. Soc.*, *114*, 281-295, 1988.
- Manney, G. L., R. W. Zurek, A. O'Neill, and R. Swinbank, On the motion of air through the stratospheric polar vortex, *J. Atmos. Sci.*, *51*, 2973-2994, 1994.
- Manney, G. L., R. Swinbank, A. O'Neill, Stratospheric meteorological conditions for the 3-12 Nov 1994 ATMOS/ATLAS-3 measurements, *Geophys. Res. Lett.*, *23*, 2409-2412, 1996.
- Manney, G. L., H. A. Michelsen, M. L. Santee, M. R. Gunson, F. W. Irion, A. E. Roche, and N. J. Livesey, Polar vortex dynamics during spring and fall diagnosed using trace gas observations from the Atmospheric Trace Molecule Spectroscopy instrument, *J. Geophys. Res.*, *104*, 18,841-18,866, 1999.
- Manney, G. L., H. A. Michelsen, F. W. Irion, G. C. Toon, M. R. Gunson, and A. E. Roche, Lamination and polar vortex development in fall from ATMOS long-lived trace gases observed during November 1994, *J. Geophys. Res.*, *105*, 29,023-29,038, 2000.
- Manney, G. L., H. A. Michelsen, R. M. Bevilacqua, M. R. Gunson, F. W. Irion, N. J. Livesey, J. Oberheide, M. Riese, J. M. Russell III, G. C. Toon, and J. M. Zawodny,

- Comparison of satellite ozone observations in coincident air masses in early November 1994, *J. Geophys. Res.*, *106*, 9923-9943, 2001.
- McCormick, M. P., E. W. Chiou, L. R. McMaster, W. P. Chu, J. C. Larsen, D. Rind, and S. Oltmans, Annual variations of water vapor in the stratosphere and upper troposphere observed by the Stratospheric Aerosol and Gas Experiment II, *J. Geophys. Res.*, *98*, 4867-4874, 1993.
- Michelsen, H. A., G. L. Manney, M. R. Gunson, and R. Zander, Correlations of stratospheric abundances of NO_y , O_3 , N_2O , and CH_4 derived from ATMOS measurements, *J. Geophys. Res.*, *103*, 28,347-28,359, 1998.
- Michelsen, H. A., C. M. Spivakovsky, and S. C. Wofsy, Aerosol-mediated partitioning of stratospheric Cl_y and NO_y at temperatures above 200 K, *Geophys. Res. Lett.*, *26*, 299-302, 1999a.
- Michelsen, H. A., G. L. Manney, C. R. Webster, R. D. May, M. R. Gunson, D. Baumgardner, K. K. Kelly, M. Loewenstein, J. R. Podolske, M. H. Proffitt, S. C. Wofsy, and G. K. Yue, Intercomparison of ATMOS, SAGE II, and ER-2 observations in Arctic vortex and extra-vortex air masses during spring 1993, *Geophys. Res. Lett.*, *26*, 291-294, 1999b.
- Michelsen, H. A., C. R. Webster, G. L. Manney, D. C. Scott, J. J. Margitan, R. D. May, F. W. Irion, M. R. Gunson, J. M. Russell III, and C. M. Spivakovsky, Maintenance of high HCl/Cl_y and NO_x/NO_y in the Antarctic vortex: A chemical signature of confinement during spring, *J. Geophys. Res.*, *104*, 26,419-26,436, 1999c.
- Michelsen, H. A., F. W. Irion, G. L. Manney, G. C. Toon, and M. R. Gunson, Features and trends in Atmospheric Trace Molecule Spectroscopy (ATMOS) version 3 stratospheric water vapor and methane measurements, *J. Geophys. Res.*, *105*, 22,713-22,724, 2000.
- Mote, P. W., K. H. Rosenlof, J. R. Holton, R. S. Harwood, and J. W. Waters, Seasonal variations of water vapor in the tropical lower stratosphere, *Geophys. Res. Lett.*, *22*, 1093-1096, 1995.
- Mote, P. W., K. H. Rosenlof, M. E. McIntyre, E. S. Carr, J. C. Gille, J. R. Holton, J. S. Kinnersley, H. C. Pumphrey, J. M. Russell III, and J. W. Waters, An atmospheric tape

- recorder: The imprint of tropical tropopause temperatures on stratospheric water vapor, *J. Geophys. Res.*, *101*, 3989-4006, 1996.
- Nedoluha, G. E., R. M. Bevilacqua, R. M. Gomez, W. B. Waltman, B. C. Hicks, D. L. Thacker, J. M. Russell III, M. Abrams, H. C. Pumphrey, and B. J. Connor, A comparative study of mesospheric water vapor measurements from the ground-based water vapor millimeter-wave spectrometer and space-based instruments, *J. Geophys. Res.*, *102*, 16,647-16,661, 1997.
- Nedoluha, G. E., R. M. Bevilacqua, R. M. Gomez, D. E. Siskind, B. C. Hicks, J. M. Russell III, and B. J. Connor, Increases in middle atmospheric water vapor as observed by the Halogen Occultation Experiment and the ground-based Water Vapor Millimeter-wave Spectrometer from 1991 to 1997, *J. Geophys. Res.*, *103*, 3531-3543, 1998.
- Newell, R. E., and S. Gould-Stewart, A stratospheric fountain?, *J. Atmos. Sci.*, *38*, 2789-2796, 1981.
- Oinas, V., A. A. Lacis, D. Rind, D. T. Shindell, and J. E. Hansen, Radiative cooling by stratospheric water vapor: Big differences in GCM results, *Geophys. Res. Lett.*, *28*, 2791-2794, 2001.
- Oltmans, S. J., and D. J. Hofmann, Increase in lower-stratospheric water vapour at a mid-latitude Northern Hemisphere site from 1981 to 1994, *Nature*, *374*, 146-149, 1995.
- Oltmans, S. J., H. Vömel, D. J. Hofmann, K. H. Rosenlof, and D. Kley, The increase in stratospheric water vapor from balloonborne frostpoint hygrometer measurements at Washington, D. C. and Boulder Colorado, *Geophys. Res. Lett.*, *27*, 3453-3456, 2000.
- Pan, L., S. Solomon, W. Randel, J.-F. Lamarque, P. Hess, J. Gille, E.-W. Chiou, and M. P. McCormick, Hemispheric asymmetries and seasonal variations of the lowermost stratospheric water vapor and ozone derived from SAGE II data, *J. Geophys. Res.*, *102*, 28,177-28,184, 1997.
- Pollock, W. H., L. E. Heidt, R. A. Luer, J. F. Vedder, M. J. Mills, and S. Solomon, On the age of stratospheric air and ozone depletion potentials in the polar regions, *J. Geophys. Res.*, *97*, 12,993-12,999, 1992.

- Pumphrey, H. C., Validation of a new prototype water vapor retrieval for the UARS Microwave Limb Sounder, *J. Geophys. Res.*, *104*, 9399-9412, 1999.
- Randel, W. J., F. Wu, J. M. Russell III, A. Roche, and J. Waters, Seasonal cycles and QBO variations in stratospheric CH₄ and H₂O observed in UARS HALOE data, *J. Atmos. Sci.*, *55*, 163-185, 1998.
- Randel, W. J., F. Wu, J. M. Russell III, and J. Waters, Space-time patterns of trends in stratospheric constituents derived from UARS measurements, *J. Geophys. Res.*, *104*, 3711-3727, 1999.
- Randel, W. J., F. Wu, A. Gettelman, J. M. Russell III, J. M. Zawodny, and S. J. Oltmans, Seasonal variation of water vapor in the lower stratosphere observed by Halogen Occultation Experiment data, *J. Geophys. Res.*, *106*, 14,313-14,325, 2001.
- Remsberg, E. E., P. P. Bhatt, and J. M. Russell III, Estimates of the water vapor budget of the stratosphere from UARS HALOE data, *J. Geophys. Res.*, *101*, 6749-6766, 1996.
- Rind, D. E., E. W. Chiou, W. Chu, S. Oltmans, J. Lerner, J. Larsen, M. P. McCormick, and L. McMaster, Overview of the Stratospheric Aerosol and Gas Experiment II water vapor observations: Method, validation, and data characteristics, *J. Geophys. Res.*, *98*, 4835-4856, 1993.
- Rind, D. E., Just add water vapor, *Science*, *281*, 1152-1153, 1995.
- Rind, D. E., and P. Lonergan, Modeled impacts of stratospheric ozone and water vapor perturbations with implications for high-speed civil transport aircraft, *J. Geophys. Res.*, *100*, 7381-7396, 1995.
- Rinsland, C. P., et al., ATMOS observations of H₂O+2CH₄ and total reactive nitrogen in the November 1994 Antarctic stratosphere: Dehydration and denitrification in the vortex, *Geophys. Res. Lett.*, *23*, 2397-2400, 1996.
- Rinsland, C. P., et al., Polar stratospheric descent of NO_y and CO and Arctic denitrification during winter 1992-1993, *J. Geophys. Res.*, *104*, 1847-1861, 1999.

- Rosenlof, K. H., A. F. Tuck, K. K. Kelly, J. M. Russell III, and M. P. McCormick, Hemispheric asymmetries in water vapor and inferences about transport in the lower stratosphere, *J. Geophys. Res.*, *102*, 13,213-13,234, 1997.
- Rosenlof, K. H., S. J. Oltmans, D. Kley, J. M. Russell III, E.-W. Chiou, W. P. Chu, D. G. Johnson, K. K. Kelly, H. A. Michelsen, G. E. Nedoluha, E. E. Remsberg, G. C. Toon, and M. P. McCormick, Stratospheric water vapor increases over the past half century, *Geophys. Res. Lett.*, *28*, 1195-1198, 2001.
- Sen, B., G. C. Toon, J.-F. Blavier, E. L. Fleming, and C. H. Jackman, Balloon-borne observations of midlatitude fluorine abundance, *J. Geophys. Res.*, *101*, 9045-9054, 1996.
- Shindell, D. T., Climate and ozone response to increased stratospheric water vapor, *Geophys. Res. Lett.*, *28*, 1551-1554, 2001.
- Siskind, D. E., and M. E. Summers, Implications of enhanced mesospheric water vapor observed by HALOE, *Geophys. Res. Lett.*, *25*, 2133-2136, 1998.
- Smith, C. A., R. Toumi, and J. D. Haigh, Seasonal trends in stratospheric water vapour, *Geophys. Res. Lett.*, *27*, 1687-1690, 2000.
- Smith, C. A., J. D. Haigh, and R. Toumi, Radiative forcing due to trends in stratospheric water vapour, *Geophys. Res. Lett.*, *28*, 179-182, 2001.
- SPARC, Assessment of upper tropospheric and stratospheric water vapour, World Climate Research Programme of WMO/ICSU, WCRP-113, WMO/TD-1043, Paris, France, 2000.
- Toon, G. C., The JPL MkIV interferometer, *Opt. Photonics News*, *2*, 19-21, 1991.
- Toon, G. C., J.-F. Blavier, B. Sen, J. J. Margitan, C. R. Webster, R. D. May, D. Fahey, R. Gao, L. DelNegro, M. Proffitt, J. Elkins, P. A. Romashkin, D. F. Hurst, S. Oltmans, E. Atlas, S. Schauffler, F. Flocke, T. P. Bui, R. M. Stimpfle, G. P. Bonne, P. B. Voss, and R. C. Cohen, Comparison of MkIV balloon and ER-2 aircraft measurements of atmospheric trace gases, *J. Geophys. Res.*, *104*, 26,779-26,790, 1999.
- Webster, C. R., R. D. May, C. A. Trimble, R. G. Chave, and J. Kendall, Aircraft (ER-2) Laser Infrared Absorption Spectrometer (ALIAS) for in situ stratospheric measurements of HCl, N₂O, CH₄, NO₂, and HNO₃, *Appl. Opt.*, *33*, 454-472, 1994.

Weinstock, E. M., E. J. Hintsa, A. E. Dessler, J. F. Oliver, N. L. Hazen, J. N. Demusz, N. T. Allen, L. B. Lapson, and J. G. Anderson, New fast response photofragment fluorescence hygrometer for use on the NASA ER-2 and the Perseus remotely piloted aircraft, *Rev. Sci. Instrum.*, *65*, 3544-3554, 1994.

Wofsy, S. C., J. C. McConnell, and M. B. McElroy, Atmospheric CH₄, CO, and CO₂, *J. Geophys. Res.*, *77*, 4477-4493, 1972.

Zöger, M., A. Engel, D. S. McKenna, C. Schiller, U. Schmidt, and T. Woyke, Balloon-borne in situ measurements of stratospheric H₂O, CH₄, and H₂ at midlatitudes, *J. Geophys. Res.*, *104*, 1817-1825, 1999.

R. M. Bevilacqua, Naval Research Laboratory, Code 7220, Washington, DC 20375.
(bevilacq@poamb.nrl.navy.mil)

E.-W. Chiou, W. P. Chu, E. E. Remsberg and C. P. Rinsland, NASA Langley Research Center, MS 401B, Hampton, VA 23681. (e.chiou@larc.nasa.gov, w.p.chu@larc.nasa.gov, e.e.remsberg@larc.nasa.gov, c.p.rinsland@larc.nasa.gov)

M. R. Gunson, F. W. Irion, G. C. Toon, J. W. Waters, and C. R. Webster, 4800 Oak Grove Dr., MS 183-601, Pasadena, CA 91109. (mrg@derecho.jpl.nasa.gov, fwi@caesar.jpl.nasa.gov, toon@mark4sun.jpl.nasa.gov, joe@mls.jpl.nasa.gov, chris.r.webster@jpl.nasa.gov)

E. J. Hintsa, MS #25, Dept. of Marine Chemistry and Geochemistry, Woods Hole Oceanographic Institution, Woods Hole, MA 02543. (ehintsa@whoi.edu)

K. K. Kelly, R/E/AL6, NOAA Aeronomy Laboratory, 325 S. Broadway, Boulder, CO 80303. (kellyk@al.noaa.gov)

G. L. Manney, Dept. of Natural Resources Management, New Mexico Highlands University, Las Vegas, NM 87701. (manney@mls.jpl.nasa.gov)

E. Mahieu and R. Zander, Inst. of Astrophysics and Geophysics, University of Liège, 4000 Liège, Belgium. (mahieu@astro.ulg.ac.be, zander@astro.ulg.ac.be)

M. P. McCormick and J. M. Russell III, Center for Atmospheric Sciences, Hampton University, P. O. Box 6075, Hampton, VA 23668. (pat.mccormick@hamptonu.edu, james.russell@hamptonu.edu)

H. A. Michelsen, Combustion Research Facility, Sandia National Laboratories, MS 9055, P.O. Box 969, Livermore, CA 94551. (hamiche@ca.sandia.gov)

M. J. Newchurch, Atmospheric Science Department, University of Alabama in Huntsville, Huntsville, AL 35899. (mike@atmos.uah.edu)

H. C. Pumphrey, Dept. of Meteorology, Univ. of Edinburgh, Edinburgh EH9 3JZ, Scotland. (hcp@met.ed.ac.uk)

P. N. Purcell, Tech Lead, Tribal DDB, NY, 437 Madison Ave., New York, NY 10022. (ppurcell@tribalddb.com)

E. M. Weinstock, Dept. of Chemistry and Biological Chemistry, 12 Oxford St., Harvard University, Cambridge, MA 02138. (elliott@huarp.harvard.edu)

¹Combustion Research Facility, Sandia National Laboratories, Livermore, California

²Jet Propulsion Laboratory, California Institute of Technology, Pasadena

³Department of Natural Resources Management, New Mexico Highlands University, Las Vegas

⁴NASA Langley Research Center, Hampton, Virginia

⁵Institute of Astrophysics and Geophysics, University of Liège, Liège-Cointe, Belgium

⁶Atmospheric Science Department, University of Alabama in Huntsville, Huntsville

⁷Tribal DDB, NY, New York

⁸Center for Atmospheric Sciences, Hampton University, Hampton, Virginia

⁹Department of Meteorology, University of Edinburgh, Edinburgh, Scotland

¹⁰Remote Sensing Division, Naval Research Laboratory, Washington, District of Columbia

¹¹NOAA Aeronomy Laboratory, Boulder, Colorado

¹²Department of Marine Chemistry and Geochemistry, Woods Hole Oceanographic Institution, Woods Hole, Massachusetts

¹³Department of Chemistry and Biological Chemistry, Harvard University, Cambridge, Massachusetts

Table 1. ATMOS Space Shuttle Missions

Mission	Dates	Latitudes	Occultation
Spacelab 3	30 April - 1 May 1985	47 - 51°S 26 - 35°N	sunrise sunset
ATLAS-1	25 March - 2 April 1992	0 - 55°S 0 - 31°N	sunrise/sunset sunrise
ATLAS-2	8 - 16 April 1993	10 - 50°S 63 - 68°N	sunset sunrise
ATLAS-3	3 - 14 November 1994	65 - 72°S 3 - 49°N	sunrise sunset

Table 2. ATMOS Optical Band-pass Filters and Species Retrievals

Filter	Wavelength region	V-2 species	Additional V-3 species
Filter 1	600 - 1180 cm ⁻¹	N ₂ O	CH ₄ , H ₂ O
Filter 2	1100 - 2000 cm ⁻¹	N ₂ O, CH ₄ , H ₂ O	
Filter 3	1580 - 3450 cm ⁻¹	N ₂ O, CH ₄ , H ₂ O	
Filter 4	3100 - 4800 cm ⁻¹	N ₂ O, CH ₄ , H ₂ O	
Filter 9	625 - 2450 cm ⁻¹	N ₂ O, CH ₄ , H ₂ O	
Filter 12	625 - 1450 cm ⁻¹	N ₂ O, CH ₄	H ₂ O

Table 3. Average Percent Differences between ATMOS-V3 and Other Instruments

Instrument	Accuracy	Lower Stratosphere 18 – 28 km	Middle Stratosphere 30 – 40 km	Upper Stratosphere 40 – 50 km	Mesosphere 60 – 70 km
NOAA Ly- α hygrometer	5-10%	-5 to +5%			
Harvard Ly- α hygrometer	5-10%	-10 to -16%			
MkIV	6%	-1 to +4%	-7 to -1%		
HALOE-V19	10-30%	0 to +7%	+1 to +6%	+3 to +8%	+4 to +19%
SAGE II-V6*	14-36%	+5 to +41%	-7 to +8%	+27 to -35%	
SAGE II-V6 [†]	14-36%	+1 to -59%	+1 to -17%	-9 to -30%	
MAS-V20	8-15%	+11 to +14%	-8 to +7%	-3 to +4%	-1 to +5%
MLS-V0104	8-25%	+12 to +22%	+7 to +14%	+1 to +9%	-1 to +14%

*Post-Pinatubo (1994)

[†]Pre-Pinatubo (1985), sunset occultations

Figure 1. Comparison of ATMOS/ATLAS-3 Version 3 retrievals of [H₂O] with NOAA Lyman- α hygrometer observations from the ASHOE/MAESA ER-2 aircraft campaign. Symbols represent in situ observations averaged in 10-K potential temperature segments of up to 1000 points with error bars representing 1 σ standard deviation of the data, and lines represent individual ATMOS profiles. The left panels (a and b) show the volume mixing ratio of H₂O plotted as a function of pressure. The middle panels (c and d) show the fractional difference between the profiles, and the right panels (e and f) display the difference between the corresponding potential vorticity profiles.

Figure 2. Comparison of ATMOS-V3 retrievals of [H₂O] with Lyman- α hygrometer observations from the SPADE ER-2 aircraft campaign. The volume mixing ratio of H₂O is plotted relative to the mixing ratio of the long-lived tracer N₂O. ATMOS observations are compared with measurements from the NOAA instrument in the left panels (a-c) and with

measurements from the Harvard instrument in the right panels (d-f). Symbols represent in situ observations averaged in 10-ppb $[\text{N}_2\text{O}]$ segments with error bars representing 1σ standard deviation of the data, and lines represent weighted averages of ATMOS profiles with error bars showing the weighted 1σ standard deviation of the mean. The SPADE data, which include observations from April 30 and May 3, 6, and 7, 1993, are sorted based on PV and $[\text{N}_2\text{O}]$. (a) and (d) SPADE data associated with vortex fragments are compared with ATMOS observations made during ATLAS-2 inside the Arctic vortex before it broke up. (b) and (e) the rest of the SPADE data from these flights with $\text{PV} > 1 \times 10^{-5} \text{ K m}^2 \text{ kg}^{-1} \text{ s}^{-1}$ are compared with ATMOS/ATLAS-2 data recorded outside the Arctic vortex. (c) and (f) The fractional differences between the ATMOS observations and those from the NOAA instrument (c) and the Harvard instrument (f) are plotted as a function of $[\text{N}_2\text{O}]$ for the vortex case (circles) and the extravortex case (squares). For the in situ data, simultaneous observations of $[\text{N}_2\text{O}]$ were provided by ALIAS.

Figure 3. Comparison of ATMOS-V3 values for $[\text{H}_2\text{O}] + 2[\text{CH}_4]$ with observations from the SPADE ER-2 aircraft campaign. Potential water ($[\text{H}_2\text{O}] + 2[\text{CH}_4]$) is plotted relative to the mixing ratio of the long-lived tracer N_2O . ATMOS observations are compared with potential water derived from ALIAS $[\text{CH}_4]$ with NOAA $[\text{H}_2\text{O}]$ in the left panels (a-c) and with Harvard $[\text{H}_2\text{O}]$ in the right panels (d-f) plotted against ALIAS $[\text{N}_2\text{O}]$. Symbols represent the in situ observations averaged in 10-ppb $[\text{N}_2\text{O}]$ segments with error bars representing 1σ standard deviation of the data, and lines represent weighted averages of ATMOS profiles with error bars showing the weighted 1σ standard deviation of the mean. The SPADE data correspond to the same data points, and the ATMOS data are from the same occultations, as shown in Figure 2 from (a) and (d) vortex air masses and (b) and (e) extravortex air masses. (c) and (f) The fractional differences between the ATMOS observations and those from the NOAA instrument (c) and the Harvard instrument (f) are plotted as a function of $[\text{N}_2\text{O}]$ for the vortex case (circles) and the extravortex case (squares).

Figure 4. Comparison of ATMOS-V3 retrievals of $[\text{H}_2\text{O}]$ and $[\text{H}_2\text{O}] + 2[\text{CH}_4]$ with MkIV observations. The volume mixing ratio of (a)-(d) H_2O and (e)-(h) potential water

($[\text{H}_2\text{O}] + 2[\text{CH}_4]$) are plotted as a function of $[\text{N}_2\text{O}]$. Symbols represent the MkIV observations, and lines represent weighted averages of ATMOS profiles with error bars showing the weighted 1σ standard deviation of the mean. (a) and (e) ATMOS observations made during ATLAS-1 at southern midlatitudes are compared with MkIV measurements from northern midlatitudes on September 14 and 15, 1992. (b) and (f) ATMOS observations made during ATLAS-2 outside the Arctic vortex are compared with MkIV measurements from northern midlatitudes on April 3, 1993. (c) and (g) ATMOS observations made during ATLAS-3 at northern midlatitudes are compared with MkIV measurements from northern midlatitudes on September 23 and 24, 1993. (d) and (h) The fractional differences between the ATMOS observations and those from the MkIV are shown for the 3 cases; symbols correspond to those used in (a)-(c) and (e)-(g). The line represents the average fractional difference.

Figure 5. Comparison of ATMOS/ATLAS-2 with MkIV observations of $[\text{H}_2\text{O}]$ and $[\text{H}_2\text{O}] + 2[\text{CH}_4]$. The left panels (a and b) show ATMOS-V3 (solid lines) and MkIV (dotted lines) values of (a) H_2O and (b) potential water ($[\text{H}_2\text{O}] + 2[\text{CH}_4]$) plotted as a function of pressure. The right panels (c and d) show the corresponding fractional differences for (c) $[\text{H}_2\text{O}]$ and (d) potential water.

Figure 6. Comparison of ATMOS/ATLAS-3 with HALOE observations of $[\text{H}_2\text{O}]$. The volume mixing ratio of H_2O is plotted as a function of pressure. The left panels (a-d) show ATMOS-V3 (solid lines) and HALOE-V19 (dotted lines) retrievals as (a) unweighted averaged profiles including ss21, ss35, ss36, ss42, ss43, ss52, ss58, ss61, ss64, and ss76 for ATMOS and a selection of HALOE profiles with similar sPV paired with each ATMOS profile and individual profiles from (b) the protovortex, (c) midlatitudes, and (d) the tropics. The middle panels (e-h) show the fractional differences between the profiles from the two instruments, including (e) the (unweighted) average fractional differences for the 10 profile pairs averaged for (a) (solid line) with error bars denoting the 1σ standard deviation of the mean difference. The right panels (i-l) show the differences between the scaled potential vorticity profiles corresponding to the measurements.

Figure 7. Comparison of ATMOS-V3 values for $[\text{H}_2\text{O}] + 2[\text{CH}_4]$ with HALOE-V19 observations. Potential water ($[\text{H}_2\text{O}] + 2[\text{CH}_4]$) is plotted as a function of pressure. The data are from the same occultations presented in Figure 6. The left panels (a-d) show ATMOS-V3 (solid lines) and HALOE-V19 (dotted lines) retrievals of potential water for (a) unweighted averaged ATMOS and HALOE profiles paired by sPV and individual profiles from (b) the protovortex, (c) midlatitudes, and (d) the tropics. (d) The middle panels (e-h) show the fractional differences between the profiles in the panels to the left (solid lines) compared with the fractional differences between the $[\text{H}_2\text{O}]$ profiles presented in Figure 6 (dashed lines). The right panels (i-l) show the $[\text{CH}_4]$ profiles used in deriving PW for ATMOS (solid lines) and HALOE (dotted lines).

Figure 8. Comparison of ATMOS/ATLAS-3 with SAGE II observations of $[\text{H}_2\text{O}]$. The volume mixing ratio of H_2O is plotted as a function of pressure. The left panels (a-d) show ATMOS-V3 (solid lines) and SAGE II-V6 (dotted lines) retrievals as (a) unweighted averages of the same ATMOS profiles shown in Figure 6 and SAGE II profiles paired with each ATMOS profile based on sPV and individual profiles from (b) the protovortex, (c) midlatitudes, and (d) the tropics. The middle panels (e-h) show the fractional differences between the profiles from the two instruments, including (e) the (unweighted) average fractional differences for the 10 profile pairs averaged for (a) (solid line) and the standard deviation of the mean difference (dotted line). The right panels (i-l) show the differences between the scaled potential vorticity profiles corresponding to the measurements.

Figure 9. Comparison of ATMOS/Spacelab 3 with SAGE II observations of $[\text{H}_2\text{O}]$. The volume mixing ratio of H_2O is plotted as a function of pressure. The left panels (a-d) show ATMOS-V3 (solid lines) and SAGE II-V6 (dotted lines) retrievals as (a) unweighted averages of 6 ATMOS profiles (ss03, ss06, ss07, ss09, ss12, and ss13) and SAGE II profiles paired with each ATMOS profile based on sPV. Individual pairs of profiles are shown in (b-d) for (b, c) northern subtropical sunsets and (d) southern midlatitude sunrises. The middle panels (e-h) show the fractional differences between the profiles from the two instruments, including (e) the (unweighted) average fractional differences for the 6 profile pairs averaged

for (a) (solid line) with error bars denoting the 1σ standard deviation of the mean difference. The right panels (i-l) show the differences between the scaled potential vorticity profiles corresponding to the measurements.

Figure 10. Comparison of ATMOS/ATLAS-3 Version 3 with MAS observations of $[\text{H}_2\text{O}]$. The volume mixing ratio of H_2O is plotted as a function of pressure. The left panels (a-d) show ATMOS-V3 (solid lines) and MAS-V20 (dotted lines) retrievals as (a) unweighted averages of the same ATMOS profiles shown in Figure 6 and MAS profiles paired with each ATMOS profile based on sPV and individual profiles from (b) the protovortex, (c) midlatitudes, and (d) the tropics. The middle panels (e-h) show the fractional differences between the profiles from the two instruments, including (e) the (unweighted) average fractional differences for the 10 profile pairs averaged for (a) (solid line) with error bars denoting the 1σ standard deviation of the mean difference. The right panels (i-l) show the differences between the scaled potential vorticity profiles corresponding to the measurements.

Figure 11. Comparison of ATMOS-V3 with MLS-V0104 retrievals of $[\text{H}_2\text{O}]$ from southern midlatitudes during 1992 and 1993. Mean (unweighted) H_2O profiles are shown as a function of pressure for MLS (dotted lines) and ATMOS (solid lines) from (a) ATLAS-1 (March 1992), and comparisons of individual profiles are shown for ATLAS-1 from (b) southern midlatitudes and (c) southern protovortex and (d) ATLAS-2 (April 1993) southern midlatitudes. The middle panels (e-h) show the fractional differences between the profiles from the two instruments, including (e) the (unweighted) average fractional differences for the 10 profile pairs averaged for (a) (solid line) with error bars denoting the 1σ standard deviation of the mean difference. The right panels (i-l) show the differences between the scaled potential vorticity profiles corresponding to the measurements. ATMOS profiles used in the mean are ss13, ss16, ss18, ss20, ss21, ss23, ss27, ss28, ss35, and ss36.

Figure 12. Percent differences between retrievals of $[\text{H}_2\text{O}]$ from ATMOS-V3 and other instruments. The percent difference is defined as $100\% * (\text{ATMOS} - \text{Other}) / (\text{Mean})$. Ranges of average percent differences are shown for several altitude ranges. The thicker lines are

used for comparisons in which the measurements were made within 6 days and 9 degrees latitude of one another. The corresponding values are given in Table 3.

Figure 1
 Top ↑
 Michelsen et al.

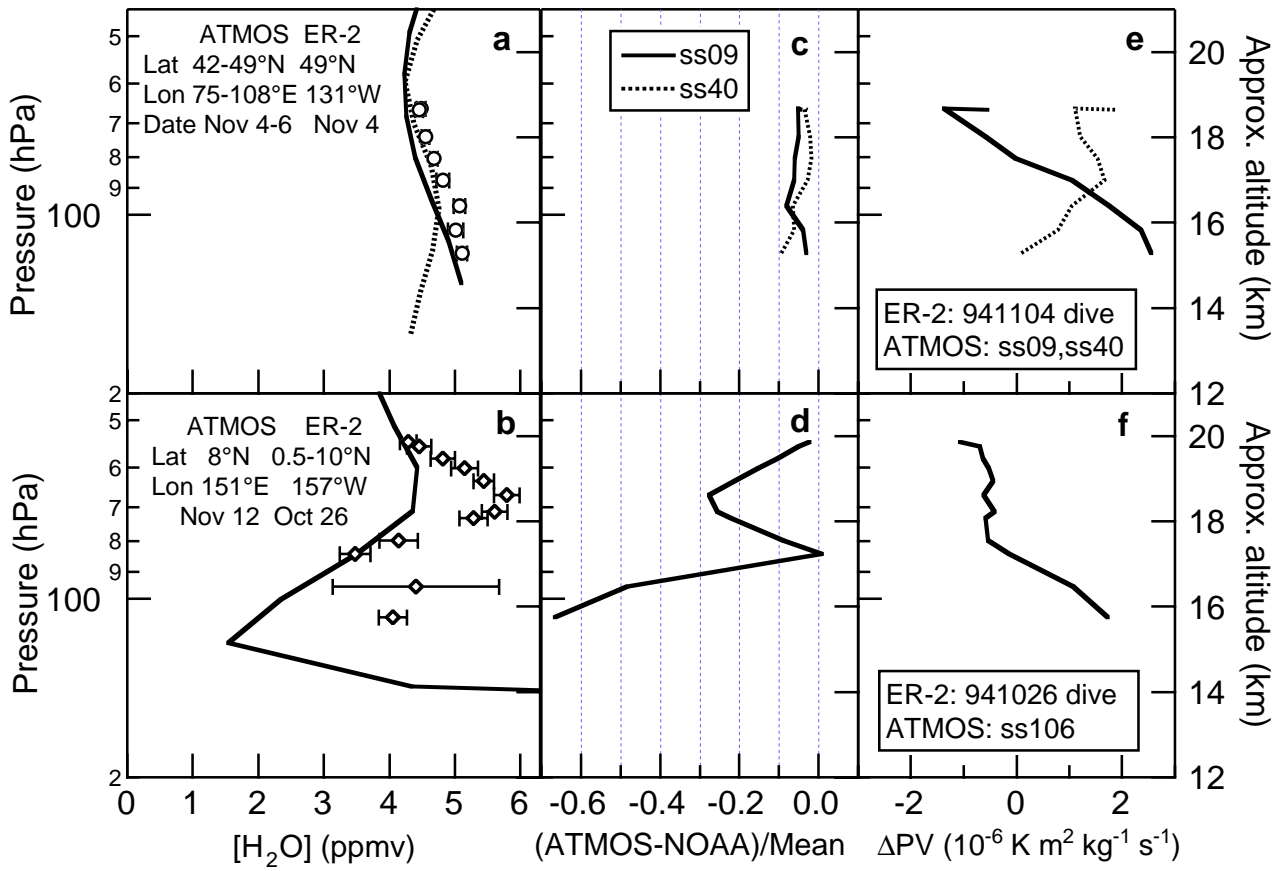


Figure 2
Top ↑
Michelsen et al.

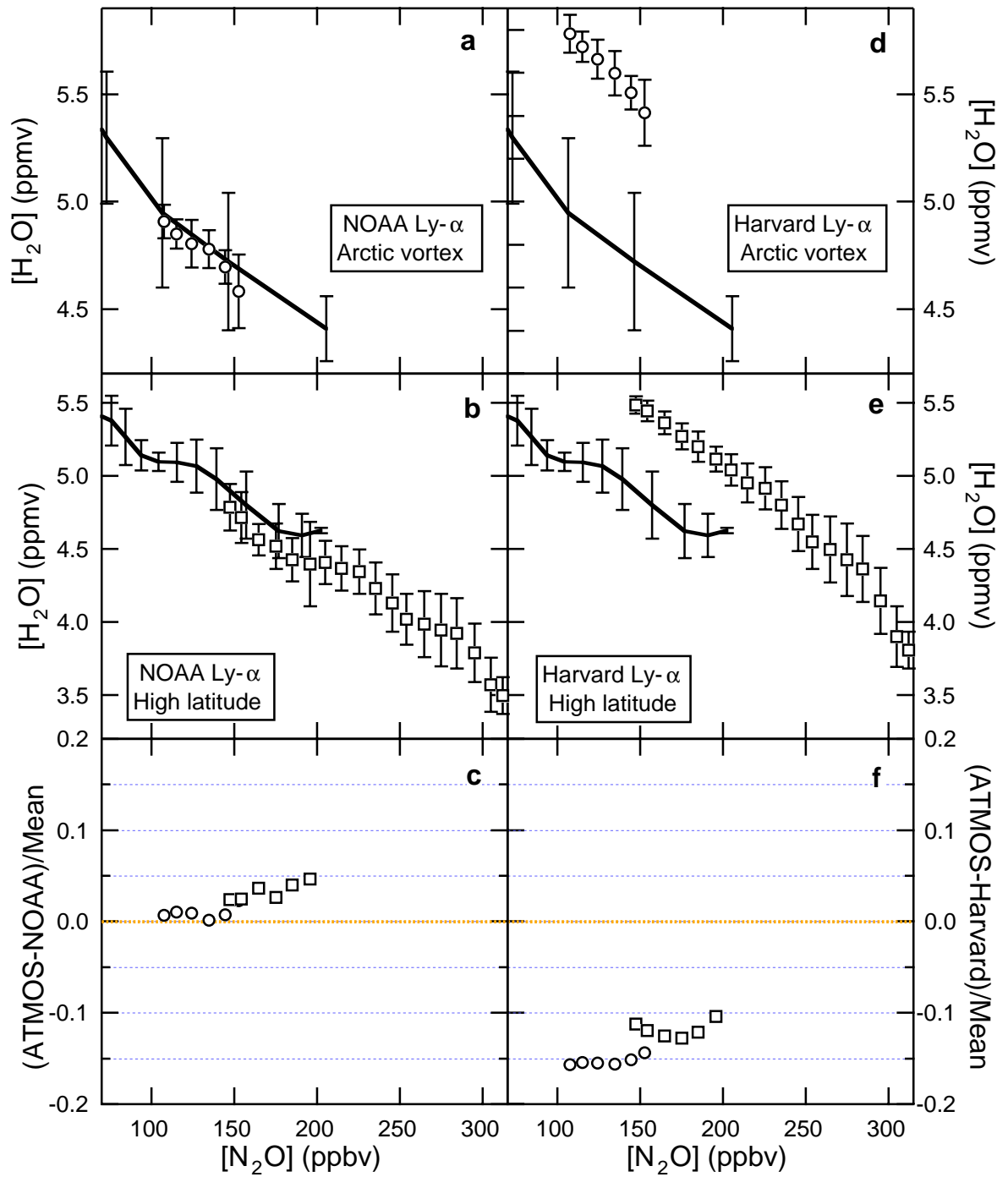


Figure 3
Top ↑
Michelsen et al.

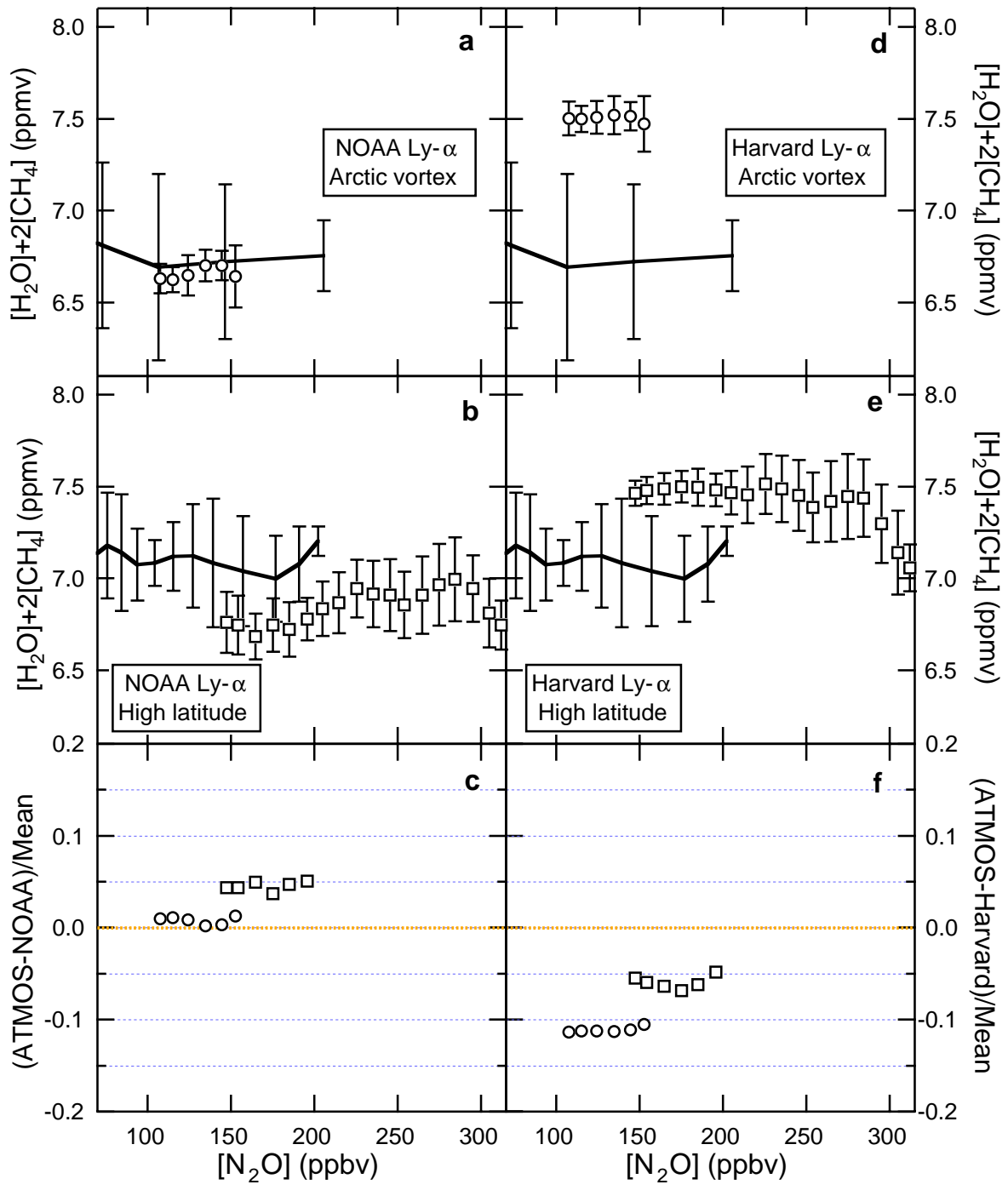


Figure 4
Top ↑
Michelsen et al.

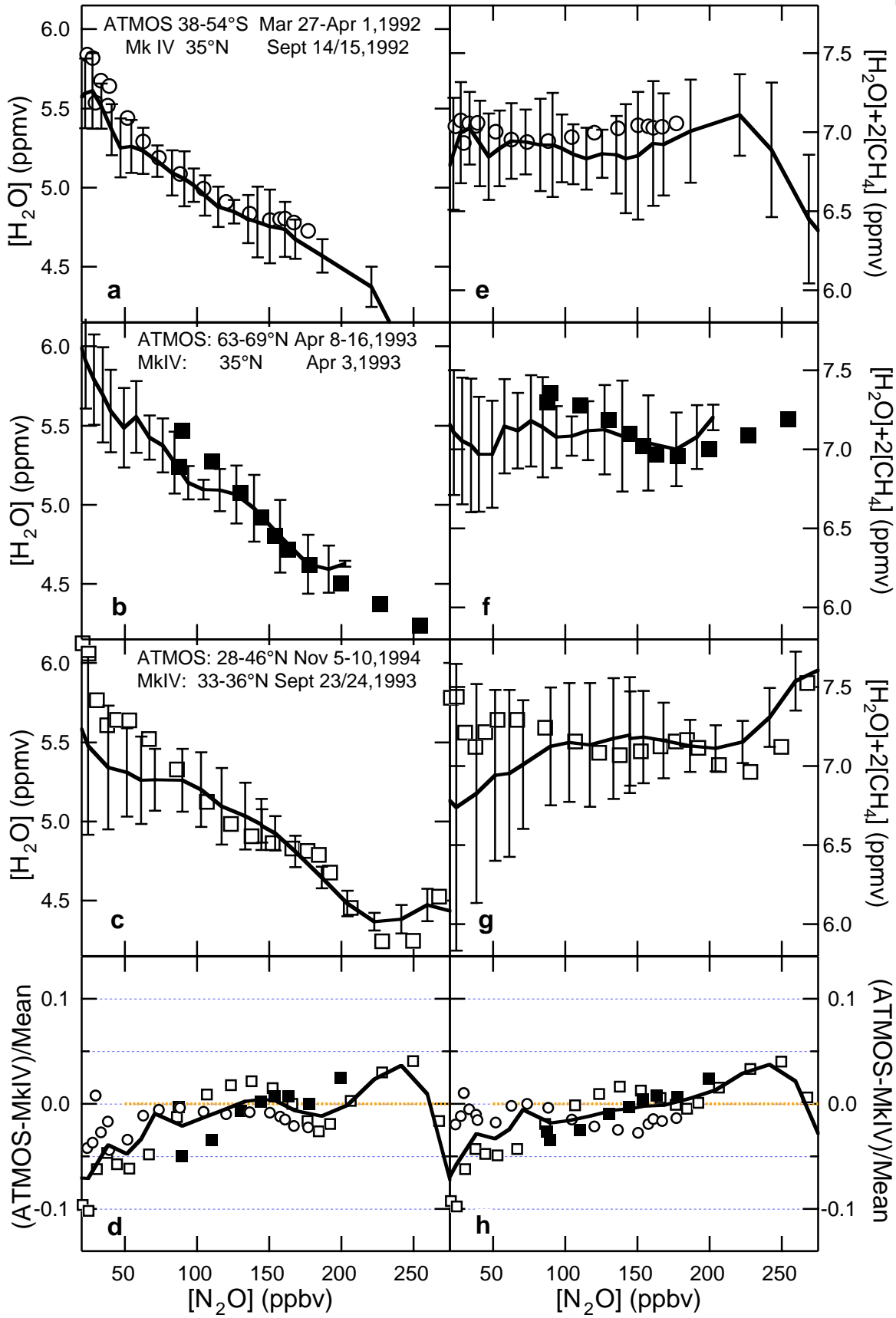


Figure 5
Top ↑
Michelsen et al.

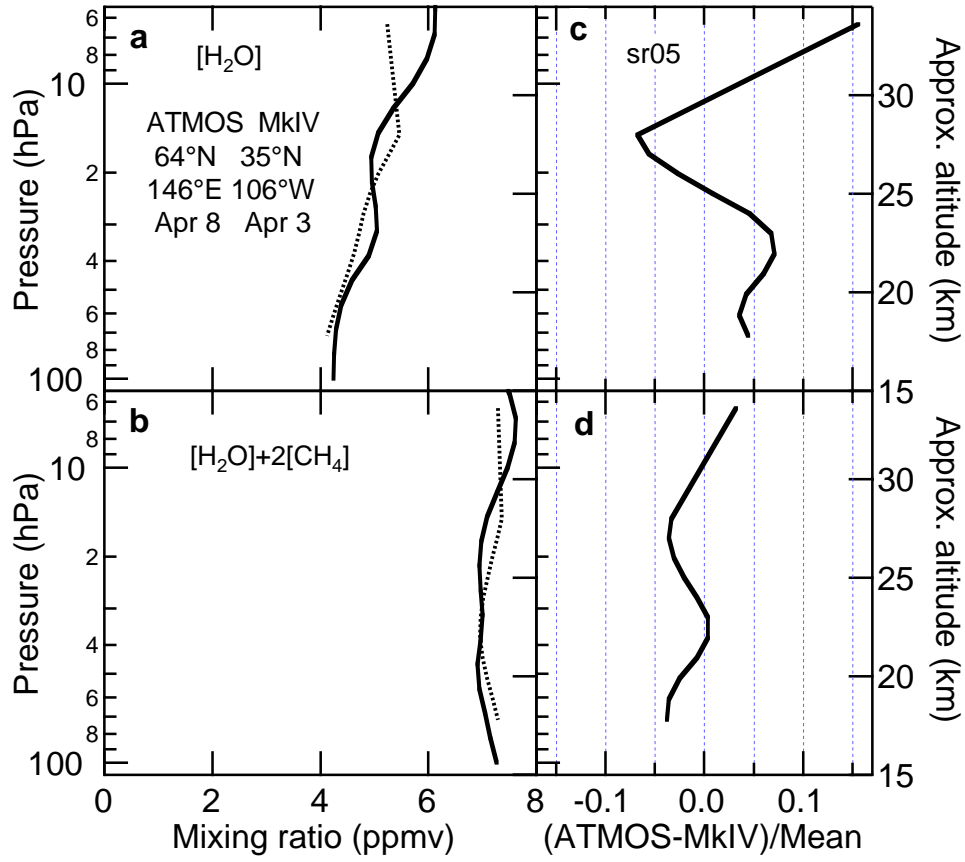


Figure 6
 Top ↑
 Michelsen et al.

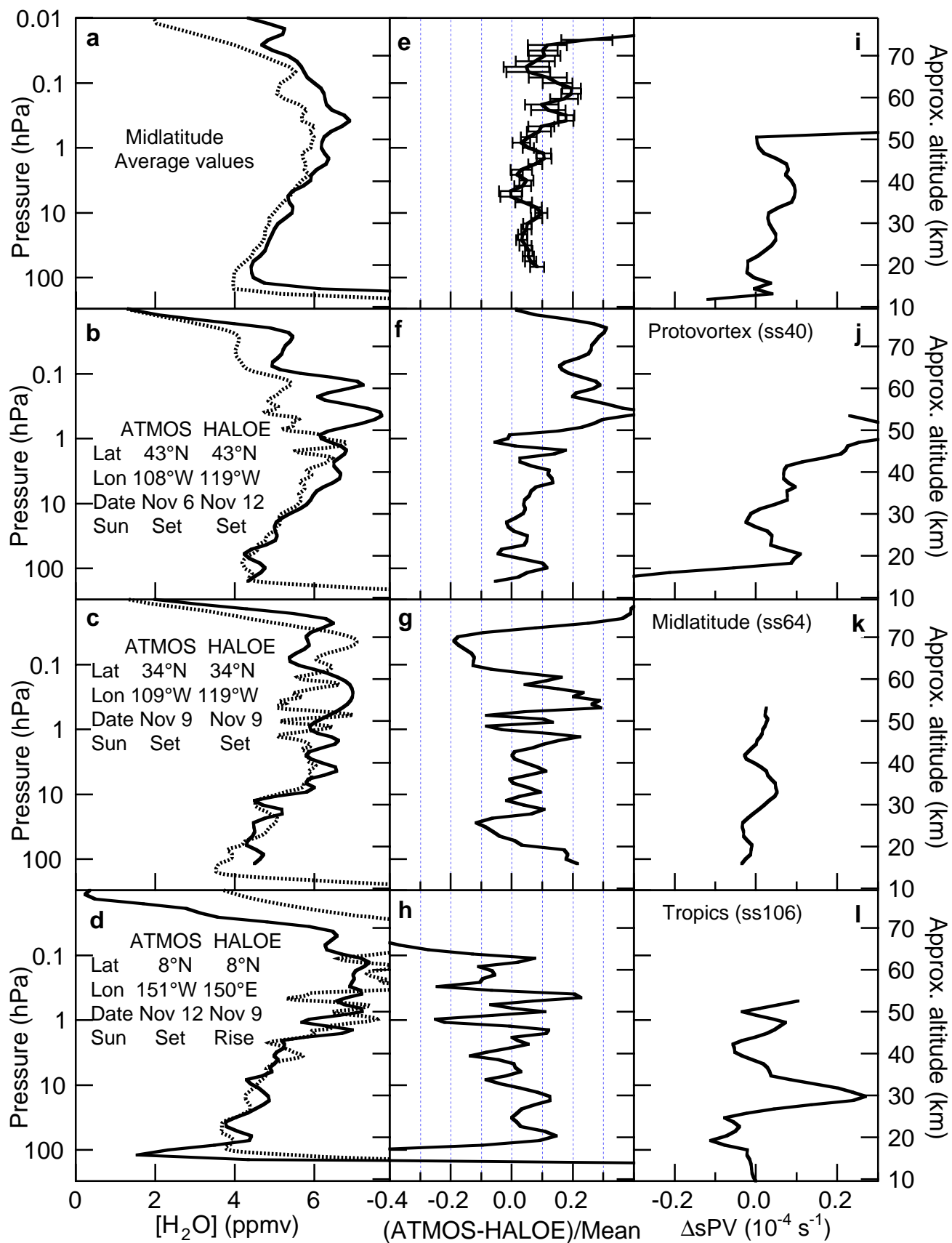


Figure 7
Top ↑
Michelsen et al.

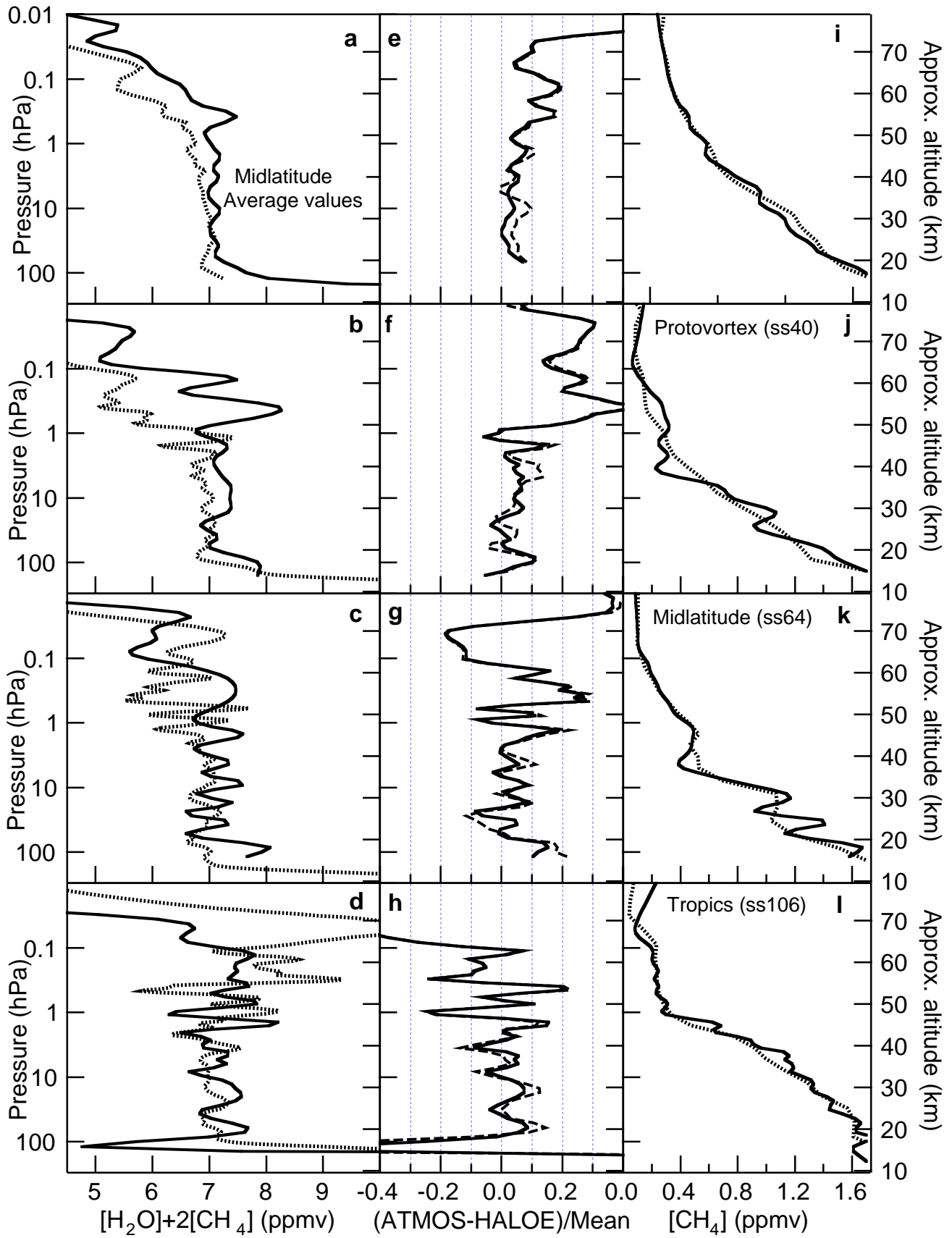


Figure 8
 Top ↑
 Michelsen et al.

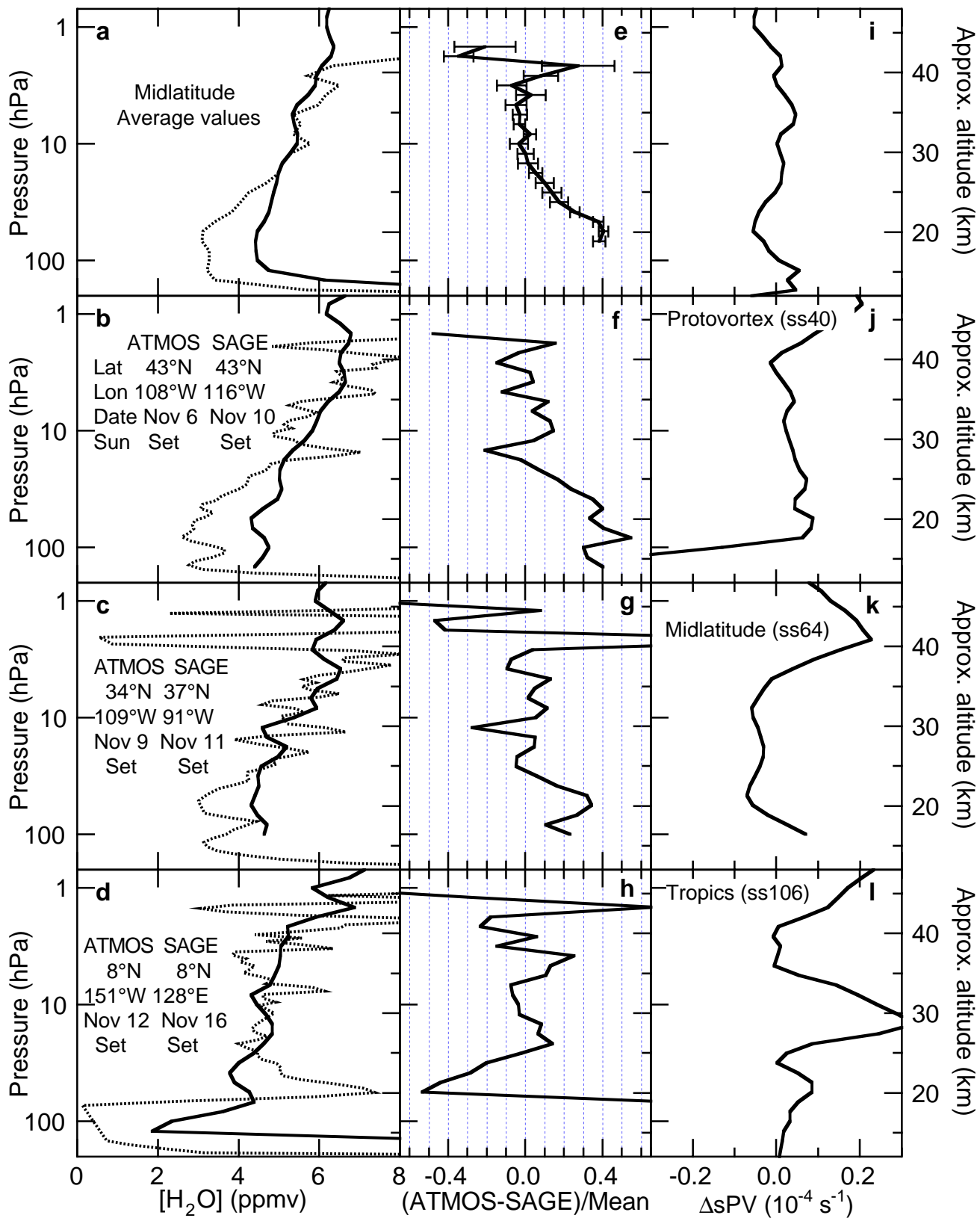


Figure 9
 Top ↑
 Michelsen et al.

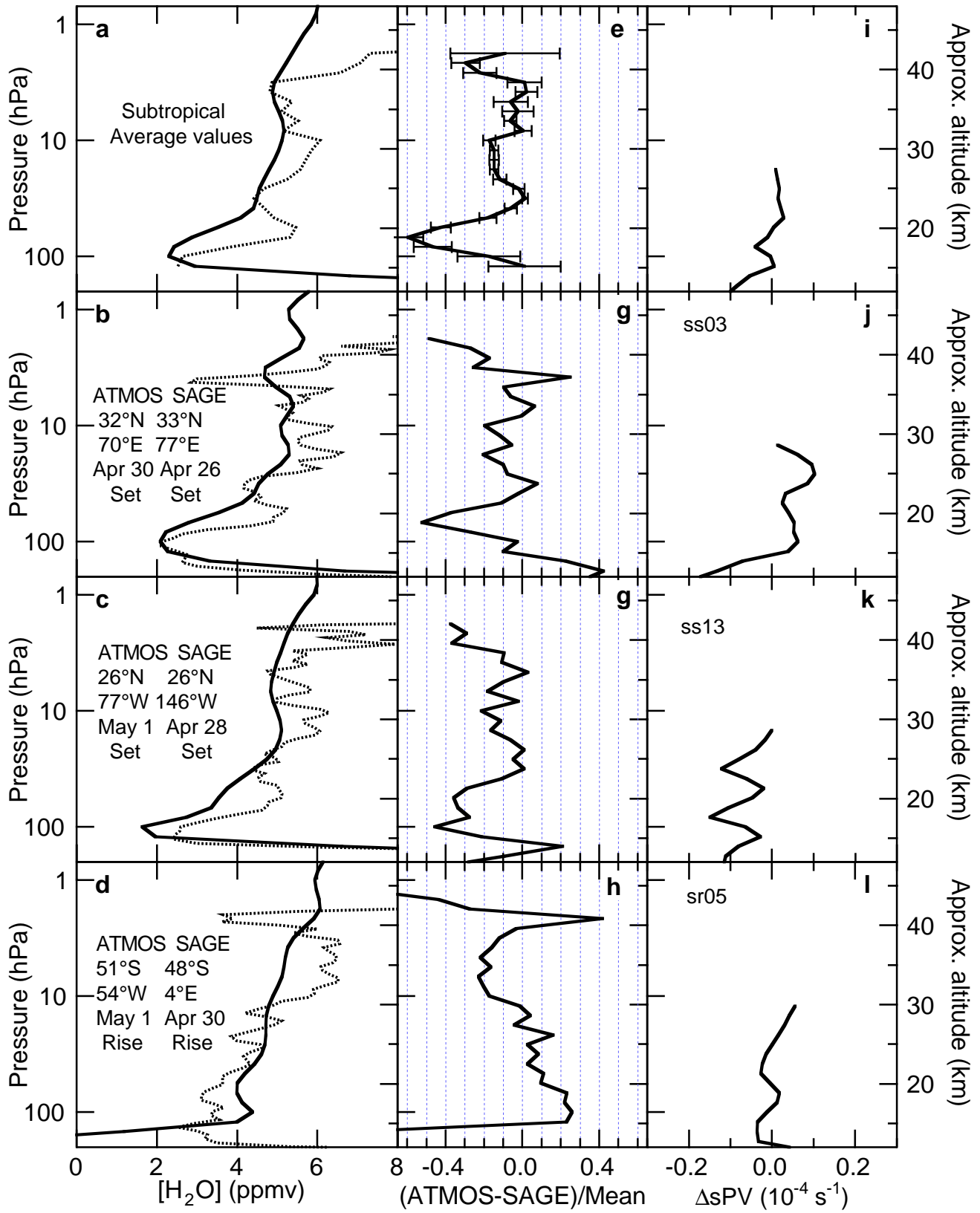


Figure 10
 Top ↑
 Michelsen et al.

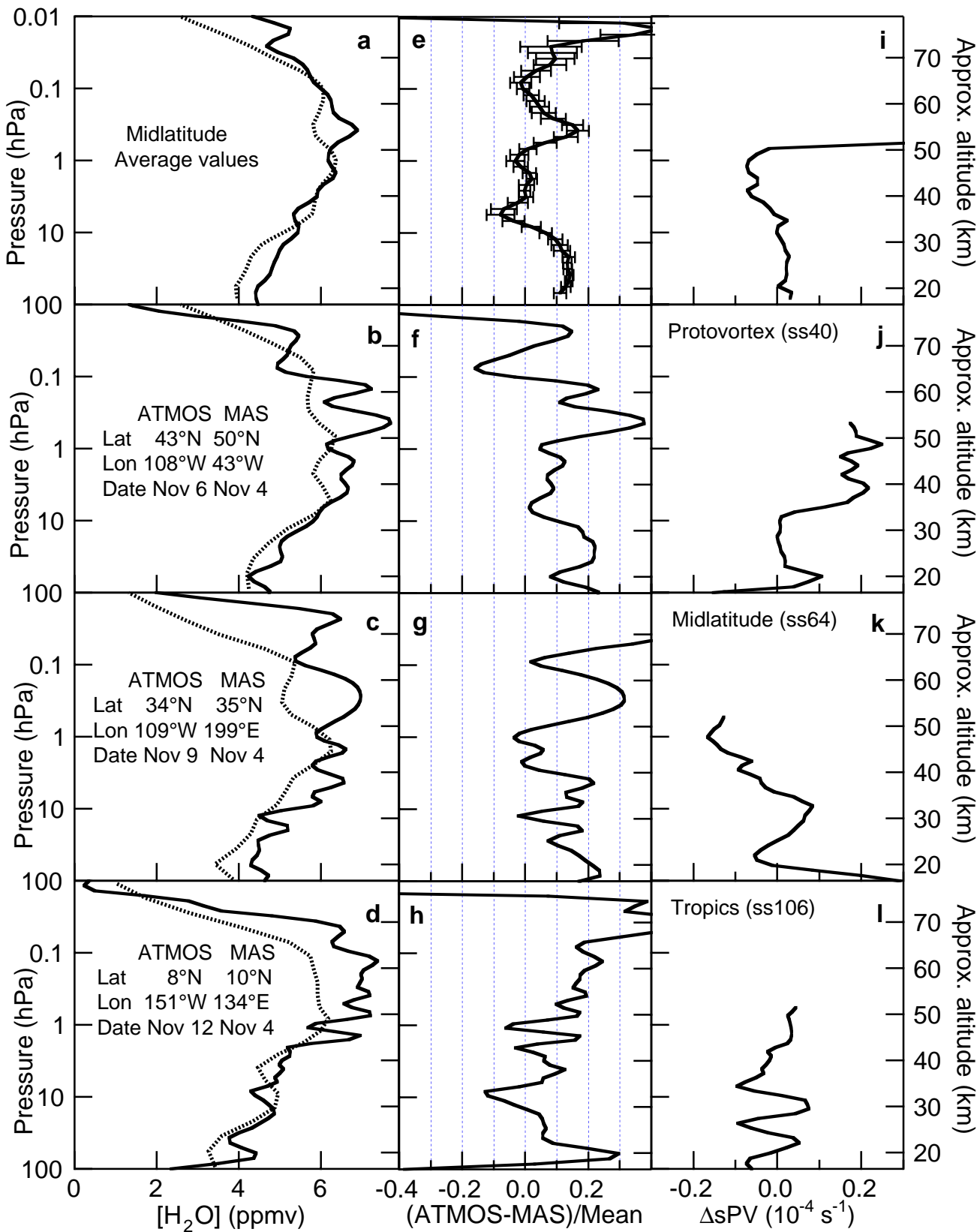


Figure 11
 Top ↑
 Michelsen et al.

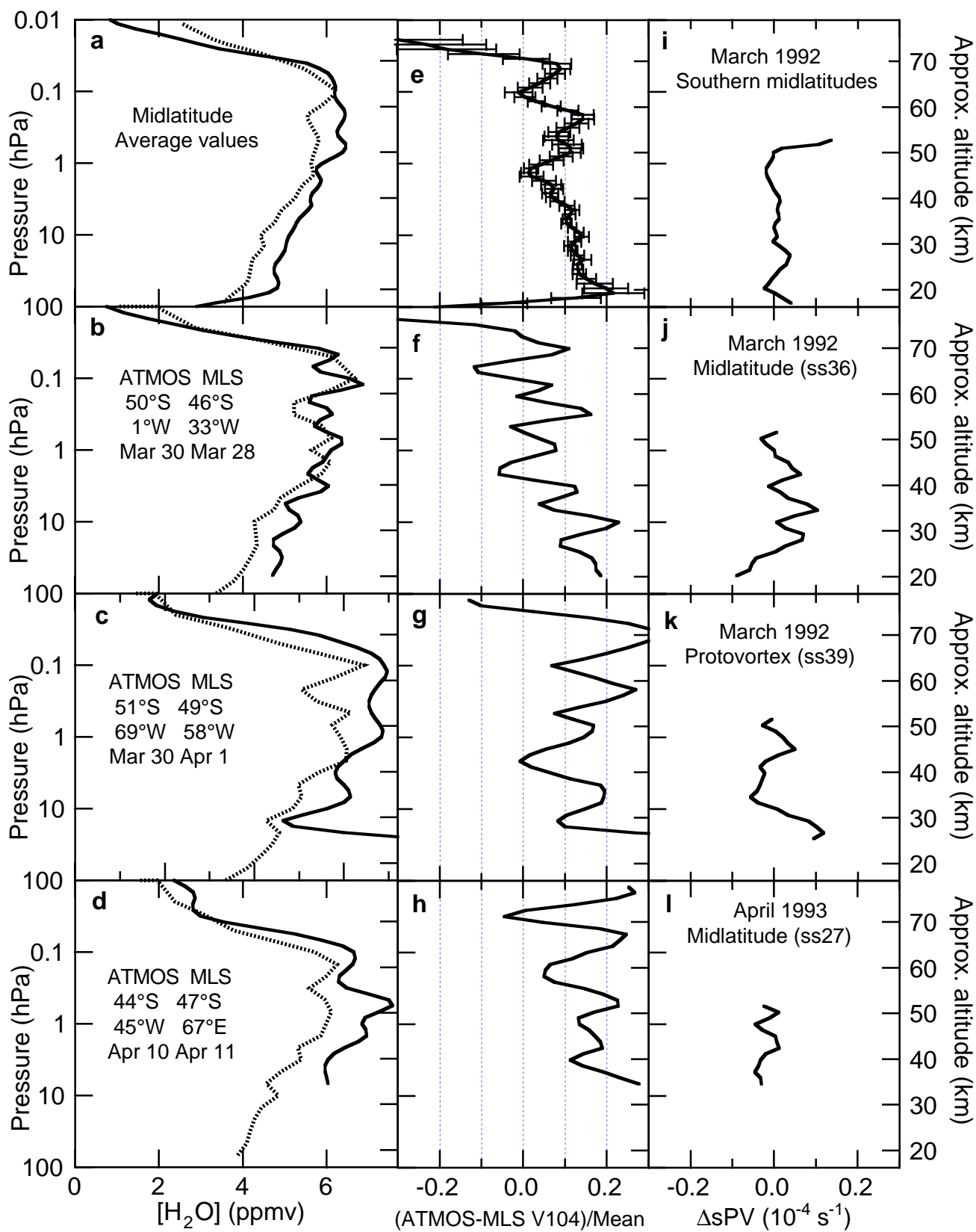


Figure 12
Top ↑
Michelsen et al.

